


History of the Giraffe Pipe locality inferred from microfossil remains: a thriving freshwater ecosystem near the Arctic Circle during the warm Eocene

Peter A. Siver*  and Anne Marie Lott

Department of Botany, Connecticut College, New London, CT, USA <pasiv@conncoll.edu>, <aliz@conncoll.edu>

Abstract.—How will freshwater lakes in the Arctic respond to climate change, especially if polar amplification results in even greater warming at these northern latitudes? Deep time analogs offer opportunities to understand the potential effects of future climate warming on arctic environments. A core from the Giraffe Pipe fossil locality located in the Northwest Territories of Canada offers a window into the life of a thriving Arctic freshwater ecosystem in the Eocene during greenhouse conditions. The remains of an extensive deposit of microfossils, including photosynthetic protists (chrysophytes, diatoms, and green algae), heterotrophic protists (euglyphids, heliozoans, paraphysomonads, and rotosphaerids), and sponges, were used to reconstruct the history of the ancient waterbody. Concentrations and diversity of chrysophyte taxa were extensive throughout the core, accounting for >70% of the microfossil remains. The ratio of chrysophyte cysts to diatom valves, with a mean value near 14 throughout the core, further emphasized the dominance of the chrysophytes, and given the high diversity of taxa, the locality represents a “paleo-hotspot” for this eukaryote lineage. Based on the totality of fossil evidence, the waterbody within the Giraffe Pipe crater represented a series of relatively shallow aquatic habitats, with changing physical and chemical conditions, and varying water depths. Five major zones were identified, each found to be stable for an extended period of time, but with distinct transitions between successive zones signaling significant shifts in environmental conditions. The study provides valuable insight on how Arctic freshwater ecosystems responded to past warm climates, and to the organisms that could potentially thrive in these environments under future warming scenarios.

Introduction

The Paleogene, especially the early to middle Eocene, represents the warmest period of the Cenozoic, when the Earth lacked a cryosphere and experienced greenhouse conditions, which could be approached again within decades to centuries given current emission trends (Tripathi et al., 2001; Zachos et al., 2001, 2008; Greenwood et al., 2010; Eberle and Greenwood, 2012; Barral et al., 2017; Westerhold et al., 2020). The onset of the Eocene was marked by an abrupt warming event known as the Paleocene-Eocene thermal maximum at 55.9 Ma (Schmitz and Pujalte, 2007; Zachos et al., 2008; Westerhold et al., 2015), and the ensuing Eocene experienced very warm temperatures relative to the modern world with additional hyperthermals at 52–50 Ma and near 42 Ma (Zachos et al., 2008).

As the twenty-first century progresses, global warming is anticipated to proceed at an unprecedented rate and, if left unchecked, result in massive reorganizations of biological systems across the planet (Kattsov and Källén, 2005; Battisti and Naylor, 2009; Richardson et al., 2011; Diffenbaugh and Field, 2013). Far greater effects are anticipated at high latitudes where significantly higher temperatures will occur relative to the global mean—a condition referred to as arctic or polar

amplification. This process is caused, in part, by positive feedback mechanisms due to reduction of Arctic sea ice, coupled with lower surface albedo, increased atmospheric water vapor, changes in cloud cover (Serreze and Francis, 2006; Lu and Cai, 2009; Screen and Simmonds, 2010; Notz and Stroeve, 2018), and shifts in circulation patterns (Ufnar et al., 2004; Seidel et al., 2008; Cohen et al., 2014). Over the last few decades the increase in arctic temperature has been twice the global average (Serreze and Francis, 2006; Screen and Simmonds, 2010; Serreze and Barry, 2011; IPCC, 2019), and models forecast a continued trend over the next century that will greatly reduce the equatorial to polar temperature gradient (Kattsov and Källén, 2005; Lunt et al., 2010, 2012).

The Eocene greenhouse had a significant effect on biogeography of plants and animals. Lush forests covered expansive land masses throughout the Arctic (Hickey et al., 1983; McIver and Basinger, 1999; Jahren, 2007; Greenwood et al., 2010; Eberle and Greenwood, 2012), numerous animals, including alligators, giant tortoises, primates, tapirs, brontotheres, and the hippo-like *Coryphodon*, roamed the landscape (Dawson et al., 1993; Eberle, 2005; Eberle et al., 2010), and the region served as a major corridor for dispersal of biota among North America, Europe, and Asia (Eberle and Greenwood, 2012). The assemblage of plants and animals in the Arctic is described as analogous to the cypress-broadleaf forests found in the southeastern U.S. (Estes and Hutchinson, 1980; Eberle and Greenwood, 2012)

*Corresponding author.

or eastern Asia (Schubert et al., 2012) today. Although shifts in species composition and biogeography in northern latitudes during the Eocene are well documented for plants (Wing et al., 1995), animals (Clyde and Gingerich, 1998; Eberle et al., 2010; Archibald et al., 2011), and even marine plankton (Sluijs et al., 2005), information on freshwater organisms is largely lacking and virtually no information is available for eukaryotic microorganisms.

Future increases in temperature, coupled with shifts in precipitation patterns, both on annual and seasonal time frames, will undoubtedly have a profound influence on Arctic freshwater ecosystems (Wrona et al., 2005; Saros et al., 2016; Colby et al., 2020). Climate changes will affect physical and chemical characteristics of aquatic systems, including the length of the growing season, stability and thermal structure, circulation patterns, duration and extent of ice cover, distribution of nutrients and dissolved gasses, concentrations of dissolved organic matter, and associated optical characteristics (Hobbie et al., 1999; Vincent and Hobbie, 2000; Wolfe, 2002; Schindler and Smol, 2006; Wrona et al., 2006; Saros et al., 2016; Hadley et al., 2019). The physical and chemical changes inevitably will affect physiological responses and adaptive strategies of organisms, composition of the biota, survival and migration patterns of species, and shifts in trophic structure. Evaluating the full range of effects potentially caused by future climate change scenarios on Arctic waterbodies will require evaluation of high latitude lakes that experienced greenhouse conditions—and therefore deep time analogs (Zachos et al., 2008; Eberle et al., 2010; Eberle and Greenwood, 2012).

The Giraffe Pipe fossil locality, situated near the Arctic Circle, offers one such deep time analog. Giraffe Pipe is a kimberlite diatreme crater that formed 48 Ma ago and harbored a freshwater environment for thousands of years, yielding an extensive and well-preserved fossil record (Siver and Wolfe, 2009; Wolfe et al., 2017). The long-term historical record, coupled with the sheer number of exceptionally well-preserved microfossils and excellent age constraints, makes the Giraffe Pipe locality perhaps the most valuable site known for elucidating shifts in biodiversity, biogeography, lake ontogeny, and ecological processes in an Arctic freshwater setting during greenhouse climates (Siver and Wolfe, 2009; Wolfe et al., 2017).

The objective of this study is to provide a high-resolution account of the changes in microorganisms, representing multiple eukaryotic lineages, found throughout the extensive core, and use the results to infer the ontogeny and history of the Giraffe Pipe waterbody. The study aims to serve as a baseline for understanding potential shifts in diversity and biogeographic patterns of freshwater microorganisms, and responses of lake ecosystems, to future warming at high latitudes.

Geologic setting

The Giraffe Pipe fossil locality (64°44'N, 109°45'W) is situated within the post-eruptive sedimentary fill of a kimberlite diatreme crater that was emplaced into the Slave Craton in the Northwest Territories of Canada during the latter part of the early Eocene (Creaser et al., 2004; Wolfe et al., 2006, 2017). After emplacement, the crater became a freshwater maar lake ecosystem, infilling over time with a sequence of lacustrine sediments, later paludal sediments, and ultimately capped by Neogene glacial deposits (Fig. 1; Siver and Wolfe, 2005a, b; Wolfe et al.,

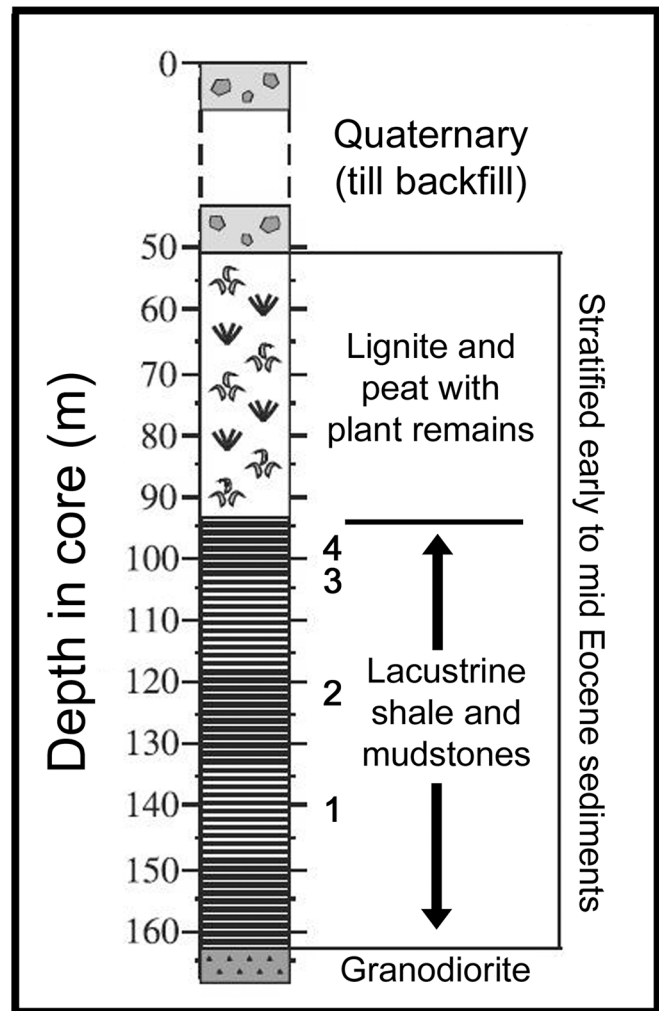


Figure 1. Stratigraphic diagram of the 163 m Giraffe Pipe core, detailing the distribution of lacustrine shales and mudstones, terrestrial plant remains, and overlying Quaternary glacial sediments. Numbers indicate the transition points between the (1) *Botryococcus* and *Aulacoseira* zones; (2) *Aulacoseira* and Eunotioid zones; (3) Eunotioid and Heterotrophic zones; and (4) the Heterotrophic and Terminal Lake zones.

2006, 2017). The waterbody formed within the crater was a small, closed basin with a diameter of 250–400 m (Wolfe et al., 2006). Wolfe et al. (2006) further noted the waterbody had elevated levels of organic material, and because of the lack of carbonates was likely a soft-water environment.

A 163 m long drilled core (Fig. 1) was recovered from the kimberlite maar in 1999 by BHP Billiton Inc. (Siver and Wolfe, 2009). A $^{87}\text{Rb}/^{87}\text{Sr}$ model age based on kimberlitic phlogopite places emplacement of the diatreme at 47.8 ± 1.4 Ma (Creaser et al., 2004). The bottom 117 m of the core contains well-preserved stratified organic sediment, including 72 m of lacustrine lake mudstones and siltstones, overlain with 45 m of terrestrial peaty material (Fig. 1). A laser-ablation inductively coupled plasma mass spectrometry $^{206}\text{Pb}/^{238}\text{U}$ estimate of zircon crystals from two tephra layers found near the end of the lacustrine deposits yielded an age estimate only slightly younger than the emplacement age (Reyes et al., 2020). These results support the idea that the 72 m of lacustrine deposits were deposited shortly after kimberlite emplacement and over a period of

thousands of years (Siver et al., 2019). Although previous studies do not suggest that any discontinuities exist within the lacustrine section of the core, including the transition points indicated in our study, we can't rule out this possibility.

Depths reported represent distances along the drilled core measured from the land surface. Core material is stored in boxes with three channels, each channel holding 1.5 m of material (4.5 m per core box). The extensive core was sub-sampled on two occasions, with 175 samples from 16 core boxes taken from the lacustrine phase spanning core depths of 168–96 m. Samples are identified using a three-part number. The first number refers to the core box, with the oldest (deepest) section of the lacustrine phase in box 26, and the termination of the lake phase in box 11. The second number identifies one of three channels within the box. The core section in channel 1 is oldest (deepest) and the section in channel 3 the youngest. The third number represents the length in cm measured from the top of the core length. For example, sample 20-1-31 represents a sample taken 31 cm from the top of the core section in channel 1 in box 20. Additional details of the Giraffe Pipe locality have been published previously (Wolfe et al., 2006, 2017; Siver and Wolfe, 2009).

Materials and methods

Preparation of samples.—Mudstone chips (0.5–1.0 g) from each of the 175 samples were oxidized using 30% H₂O₂ under low heat for a minimum of an hour and rinsed multiple times with distilled water. The resulting slurry was brought to 10 ml with distilled water and stored at 4°C in glass vials. This oxidation procedure was sufficient to separate microfossils from the rock matrix for most samples. If needed, some samples also were oxidized with a sulfuric acid-potassium dichromate solution (Marsicano and Siver, 1993). A 0.5 ml aliquot of each slurry was diluted with 2 ml of distilled water and air dried onto a piece of heavy duty aluminum foil, and onto four circular glass coverslips. If the microfossil remains on the aluminum foil and coverslips were too concentrated, the dilution step was redone, most often with 4 ml of distilled water. The aluminum foil samples were trimmed, attached to aluminum SEM stubs with Apiezon® wax, coated with a mixture of gold and palladium for 2 min with a Polaron Model E sputter coater, and observed with either a Leo 982 or an FEI Nova field emission scanning electron microscope. The coverslips were mounted onto glass slides using Naphrax, and examined with an Olympus BX-51 or Leica DMR light microscope. Counts were done on the Olympus BX-51.

Identification and enumeration of microfossils.—Except for fossilized colonies of the green alga, *Botryococcus*, all microfossils were siliceous in nature, including cysts, scales and bristles of chrysophyte taxa, scales of heliozoans and other heterotrophic protists, plates of testate amoebae, spicules from freshwater sponges, and valves or frustules of diatoms. Chrysophyte cysts were separated into two size categories, specimens with diameters $\leq 10 \mu\text{m}$ and those $> 10 \mu\text{m}$. Chrysophyte scales were identified to species for all genera except those belonging to *Paraphysomonas* and *Lepidochromonas*, which were grouped together and referred to as “paraphysomonads.” Heliozoan scales (including plate and

spine scales) were separated into four groups, each representing remains of taxa within a given genus: *Raphidiophrys*, *Acanthocystis*, *Choanocystis*, and *Raineriophrys*. Remaining heterotrophic scales enumerated belonged to rotosphaerids, specifically the genus *Rabdiophrys*. Testate plates were separated into three groups according to Barber et al. (2013), including those that are shield-shaped with bilateral symmetry (belonging to the genus *Scutiglypha*), those that are circular to oval (largely belonging to the genus *Euglypha*), and those plates with square to rectangular morphologies (multiple genera). Sponge spicules were divided into megascleres, microscleres, and gemmulescleres. Diatom remains were identified to genus and/or species, but for analysis, the final counts were lumped into four groups: centrics (e.g., consisting mostly of *Aulacoseira* spp.); eunotioids (*Eunotia* spp. and *Actinella* spp.); araphid pennates (e.g., *Oxyneis* spp., *Fragilaria* spp., *Fragilariforma* spp., and *Ambistria*); and raphid pennates (e.g., *Nupela*). Numerous phytoliths and pollen grains also were enumerated, but not included in the analyses.

Organisms in each sample were enumerated using a combination of scanning electron microscopy (SEM) and light microscopy (LM). Because the sizes of microfossils identified and enumerated for this study covered a wide range, counts were done at multiple magnifications (40× and 100×) for each sample, and later assembled into a combined database. Four steps were used to quantify the organisms in each sample.

First, each sample was first thoroughly investigated with scanning electron microscopy (SEM) in order to identify, estimate the relative abundance of, and image each organism. Remains of almost all of the organisms identified with SEM then could be recognized and enumerated with LM. However, it was not possible to count the small scales of paraphysomonads with LM, therefore paraphysomonad scales were counted from a random number of fields with SEM, along with a known number of chrysophyte cysts. The ratio of paraphysomonad scales to cysts established with SEM was used to estimate the number of paraphysomonad scales in each LM count based on the number of cysts in the count. For example, if the SEM analysis yielded two paraphysomonad scales for each cyst, and there were 10 cysts in a final count made with LM, then 20 paraphysomonad scales were added to the LM count. This same ratio method was used to estimate the number of *Botryococcus* colonies per LM count.

Second, after SEM investigation, organisms in each sample were enumerated with LM at both 40× and 100× using the same prepared slide. All larger microfossils were enumerated in a known number of fields along a horizontal transect made midway on the coverslip. These included sponge spicules, diatom valves, chrysophyte cysts, and testate plates. At least 300 microfossils were counted. If additional microfossils needed to be counted, fields were selected along a vertical transect midway on the slide. This procedure was then repeated at 100× to enumerate a minimum of 300 chrysophyte, heliozoan, and other heterotrophic protist scales.

Third, a stage micrometer was used to measure the diameter of a field at both 40× and 100×, and these measurements used to calculate the area of a field at each magnification. The surface area of a field viewed under 40× is 7.6× larger than a field viewed at 100×. This statistic was used to transfer counts per field made

Table 1. The most abundant taxa uncovered and enumerated in 175 samples taken from the Giraffe Pipe core. Data include the percentage of the total microfossils counted across all samples, the number of samples where the taxon accounted for >50% of the total count, and the maximum percentage within any single sample. Percentages of the total microfossils counted are also given after removing all Chrysophyceae taxa. Organisms are grouped as autotrophs or heterotrophs. Key: “C.” = *Chrysosphaerella*; “M.” = *Mallomonas*; “S.” = *Synura*.

Taxon	% of total microfossils counted	# samples accounting for >50%	Maximum % in a given sample	% of total microfossils minus chrysophytes
Autotrophs				
Chrysophyte cysts	13.6	41	100	NA
<i>Chrysosphaerella</i> sp.	1.2	1	56.2	NA
<i>M. asmundiae</i> (Wujek and Van DerVeer, 1976) Nicholls, 1982	4.6	6	75.7	NA
<i>M. insignis</i> Penard, 1919	18.6	8	91	NA
<i>M. lychenensis</i> Conrad, 1938	15.8	12	92.8	NA
<i>M. porifera</i> Siver and Wolfe, 2005b	3.5	3	70.6	NA
<i>M. schumachii</i> Siver, 2015	1.9	2	78.8	NA
<i>S. cronbergiae</i> Siver, 2013	7.1	2	71.9	NA
<i>S. nygaardii</i> (Petersen and Hansen, 1956) Kristiansen, 1997	7.1	2	80.9	NA
<i>S. recurvata</i> Siver and Wolfe, 2005b	2.0	0	36.0	NA
Eunotioid diatoms	2.7	1	56.2	15.3
Centric diatoms	5.2	6	77.2	29.1
<i>Botryococcus</i> colonies	0.31	5	100	1.8
Heterotrophs				
Testate plates	0.71	0	20.8	4.0
Sponge spicules	0.41	0	10.1	2.3
<i>Rabdiophrys</i> sp.	2.7	1	50.2	15.2
Heliozoan scales	4.4	2	62.0	27.4
Paraphysomonad scales	0.9	3	71.6	*4.8

*Even though this taxon is a heterotrophic Chrysophyceae, it is lumped with the non-chrysophytes for this calculation.

at 40× to counts per field as if counted at 100×. The resulting database contained estimates of the numbers of each taxon per field at 100×.

Fourth, counts of paraphysomonads and *Botryococcus* colonies estimated with SEM were next added to the database by using the number of microfossils per chrysophyte cyst statistic. By knowing the numbers of microfossils per chrysophyte cyst in a count made with SEM, and the number of cysts per field made with LM, estimates of the abundances of organisms made with SEM were added to the database. Chrysophyte cysts were used to relate the SEM and LM counts because they were readily identified with either SEM or LM. After the estimates of the numbers per field for organisms made with SEM were added, the final database was used to calculate the relative percentages of all taxa in each sample.

Analyses of samples.—All cluster, non-metric multidimensional scaling (nMDS), SIMPROF tests for significance, and similarity percentage analyses (SIMPLER) were done using the software package Primer-E (ver. 7.0.12, Clarke and Warwick, 2001; Clarke et al., 2014). Initial cluster and non-metric multidimensional scaling (nMDS) analyses were performed based on the mean abundances of microfossil taxa in all samples from each core box. For these analyses, mean values were calculated for each microfossil taxon across all samples from a given core box using the Averaging tool in Primer-E. The data were $\log_e(X + 1)$ transformed, and a Resemblance matrix formed using a Bray-Curtis statistic. Next, a cluster analysis using group-average linkage with a SIMPROF test was performed on the Resemblance matrix, yielding groups of statistically significant samples (core boxes) based on the microfossil abundances. A SIMPROF test detects significant nodes (groups) within the cluster analysis. The nMDS

ordination was also performed on the Resemblance matrix, and visually illustrated to include the significant groupings identified in the cluster analysis. These initial analyses provided an excellent overview of the major ontological zones that occurred over the history of the Giraffe Pipe waterbody.

Cluster and nMDS analyses were next performed using the full set of 175 samples (no averaging by box). The overall results of these analyses largely mirrored those observed using the averages within each core box, but were further used to fine-tune sample assignments to specific lake zones. For example, the initial analyses based on box averages identified a significant zone that existed early in the history of the lake, and shifted abruptly to another zone represented by samples in boxes 20–17, with the transition occurring between boxes 21 and 20. The analysis using the full set of samples identified the transition to occur within the lower section of box 20, and was used to identify the samples in the older section of that box that grouped with samples in box 21 and below (i.e., the lower section of the lake). This procedure allowed for fine-tuning the transition points between the major lake zones identified throughout the lacustrine phase of the core. The results of these analyses identified five major zones, the first four named after one or more of the important taxa within the zone: *Botryococcus* Zone, *Aulacoseira* Zone, Eunotioid Zone, Heterotrophic Zone, and the Terminal Lake Zone.

Each of the 175 samples was then scored according to the appropriate lake zone and the SIMPER routine in Primer used to identify sets of taxa that best characterize the community structure within and between the major lake zones. SIMPER, similarity percentage analysis, identifies the taxa contributing the most to the overall average dissimilarity between zones. The average of the Bray-Curtis dissimilarities between all pairs of samples in any two lake zones is calculated, and the

contribution of each organism estimated. In addition, the ratio of the average contribution of a taxon divided by the standard deviation of the contributions across all pairs of samples making up the average (Avg/SD) was calculated for each contributing taxon. Taxa with higher Avg/SD scores represent better discriminating organisms. The SIMPER analysis was performed between all pairs of successive lake zones (e.g., *Aulacoseria* and Eunotioid zones).

Two additional calculations were made. First, the percentages of microfossils representing heterotrophic (as opposed to autotrophic) organisms versus depth were calculated for each sample based on the taxon assignments given in Table 1. Second, the number of chrysophyte cysts to diatom valves was also calculated for each sample. All but one of the 175 samples contained cysts. However, more samples lacked diatoms, and most of these samples had ample numbers of cysts. In order to include these samples in the plot of the ratio of cysts to diatoms versus depth, we added one diatom to the count.

Qualitative changes in the core lithology.—Qualitative changes in the sections of the core associated with each major lake zone determined through analysis of the microfossil remains, and the transitions between successive zones, were studied using photographic images of the core taken at the time the core was sub-sampled. This analysis was done post priori of the lake zone determinations based on the microfossil remains.

Repositories and institutional abbreviations.—The core taken by BHP Billiton Inc. from the Giraffe Pipe locality is archived at the Geological Survey of Canada's core and cuttings repository in Calgary, Alberta, Canada. All samples taken from the core and used in this study are archived at the Connecticut College core facility, New London, Connecticut, U.S.A. Types and type material for all organisms originally described from the Giraffe Pipe locality are archived at the Canadian Museum of Nature (CMN).

Results

Identification and stratigraphy of organisms.—Microfossil specimens ($n = 75,000$) representing seven major lineages and 58 taxa were identified and enumerated for all 175 samples (Supplemental Table S1). Microfossils ranged in size from $<1 \mu\text{m}$ (e.g., scales of paraphysomonads) to $>200 \mu\text{m}$ (e.g., sponge spicules), and the mudstone rocks contained high concentrations of well-preserved microfossils throughout the core (e.g., Fig. 2). Although some of the organisms have been described or reported previously, representatives of taxa found especially important for characterizing the major lake zones are listed in Table 1 and illustrated in Figure 3. In general, microfossils representing the Chrysophyceae (including the Synurales) dominated the majority of samples throughout the core, accounting for 72% of the total microfossils enumerated. Chrysophyte specimens included cysts (e.g., Fig. 3.2), scales (e.g., Fig. 3.3, 3.5–3.9, 3.13, 3.18), and bristles, however only the former two structures were included in the enumerations. Other core intervals were dominated or co-dominated by remains of siliceous plate-bearing testate amoebae (e.g., Fig. 3.11, 3.12), heliozoans (e.g., Fig. 3.15–3.17), diatoms (e.g.,

Fig. 3.1, 3.14), heterotrophic rotosphaerids (e.g., Fig. 3.19), and/or the chlorophyte, *Botryococcus* (Fig. 3.4). Remains of sponge spicules (e.g., Fig. 3.10) representing the family Spongillidae, and to a lesser extent family Potamolepidae, were found throughout the core, but in low numbers in most samples.

Thirty-eight of the taxa belonged to the Synurales, including 33 *Mallomonas* and five *Synura* taxa (Supplemental Table S1). Based on scale morphology, all but one would be classified at the species level. One taxon, referred to here as *Mallomonas lichenensis* Conrad, 1938, contains scale types that likely represent up to three closely related species. The majority of diatoms belonged to *Aulacoseira giraffensis* Siver, Wolfe, and Edlund in Siver et al., 2019 (Fig. 3.14), the most abundant species in the centric diatom category, or to the eunotioids, the latter comprised of multiple species belonging to the genera *Eunotia* and *Actinella* (e.g., Fig. 3.1). Remains of araphid diatoms accounted for only 0.4% of the specimens enumerated, but were of minor importance in specific sections of the core. The majority of raphe-bearing specimens other than the eunotioids belonged to *Nupela mutabilis* Siver, Wolfe, and Edlund, 2010. Other than *A. giraffensis*, additional taxa that grouped within the centric diatom category included several cyclotelloid taxa (Wolfe and Siver, 2009) and rarer *Aulacoseira* spp. (Siver, 2021).

Testate amoebae plates were common throughout the core (found in 159 of the 175 samples) and accounted for 4% of the non-chrysophyte microfossils (Table 1). Taxa with circular or oval plates (largely *Euglypha* spp., Fig. 3.11), and those with bilateral and shield-like plates (*Scutiglypha* spp., Fig. 3.12), were the most common testate species, while specimens with square to rectangular (multiple genera) plates were of minor importance. Remains of heliozoans (e.g., Fig. 3.15–3.17) also were found throughout much of the core, accounting for 27.4% of the non-chrysophyte microfossils (Table 1), and grouped into four categories based on similarities in scale morphology with known genera: *Raphidiophrys*, *Acanthocystis* (Fig. 3.16), *Choa-nocystis* (Fig. 3.15), and *Raineriophrys* (Fig. 3.17). The last two microfossil groups included plate (Fig. 3.19) and spine scales belonging to the heterotrophic protist *Rabdiophrys*, and colonies of the green alga *Botryococcus* (Fig. 3.4).

Stratigraphic distributions of taxa within the core (e.g., Fig. 4) can be divided into four general patterns. Some microfossil groups, for example chrysophyte cysts (Fig. 4.1), were more or less evenly distributed throughout the core. Other taxa, such as testate amoebae, also were recovered over most of the core, but significantly more abundant within specific sections (Fig. 4.2). Many organisms were restricted to specific sections of the core, spanning from less than one to several meters. Lastly, groups of taxa dominated larger segments of the core spanning from five to over 20 m sections.

Sixteen taxa were identified as most significant (see below) in characterizing major shifts in community structure over the lifetime of the Giraffe Pipe waterbody. *Botryococcus* was abundant in the lower sections of the core between 169–140 m, corresponding to core boxes 26–21 (Fig. 4.3). Four other taxa, *Chryso-sphaerella*, paraphysomonads, *Raineriophrys* heliozoans, and testate amoebae, were also common to abundant in lower (older) sections of the core, as well as in upper (younger) strata. *Chryso-sphaerella* (Fig. 4.15) was an important component of the community between 154–149 m (box 23), and

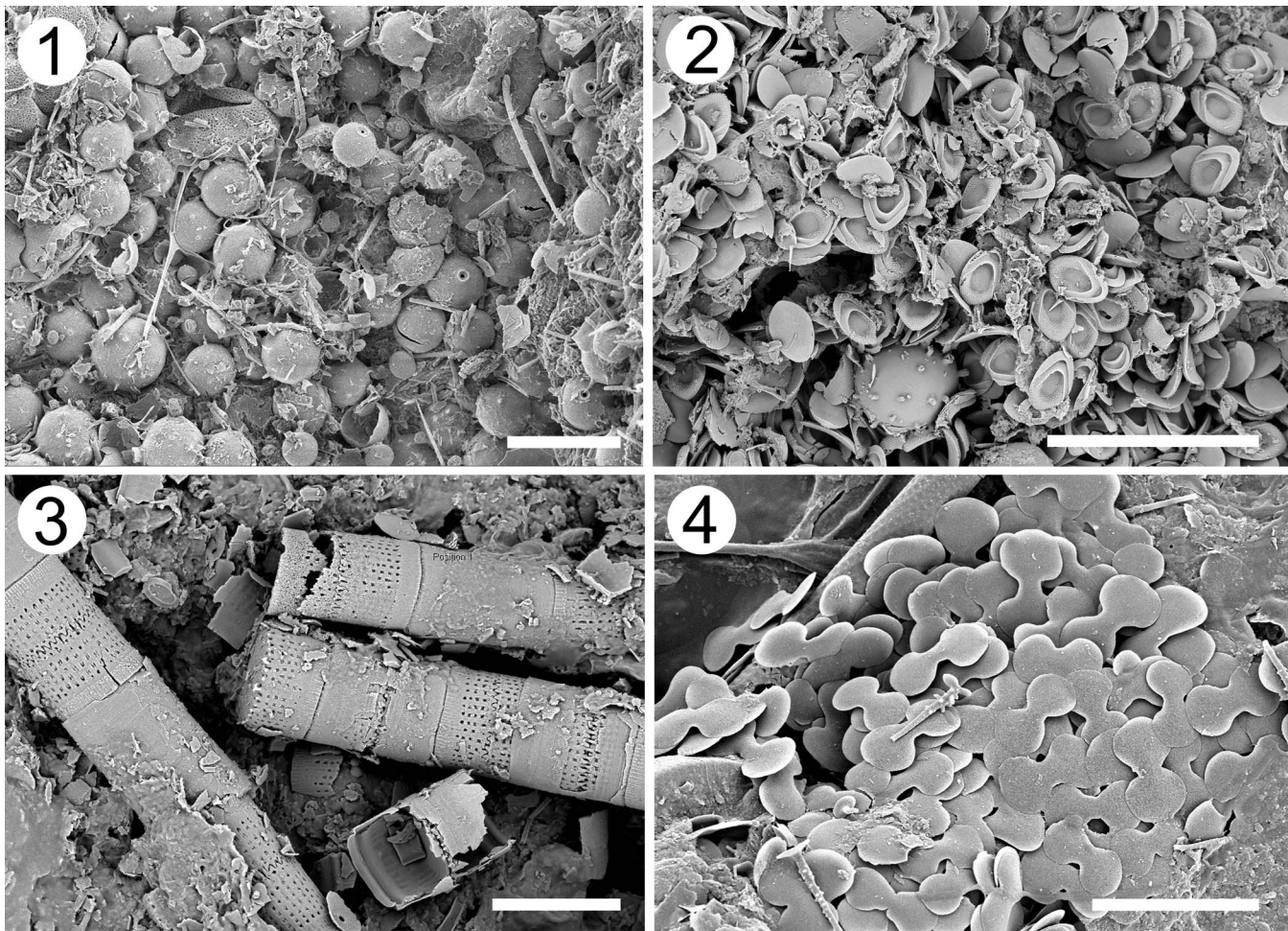


Figure 2. Scanning electron micrographs of untreated rock fragments from four representative stratigraphic intervals of the Giraffe Pipe core dominated by (1) chrysophyte cysts; (2) scales of *Mallomonas insignis* Penard, 1919; (3) the diatom *Aulacoseira giraffensis* Siver, Wolfe, and Edlund in Siver et al., 2019; and (4) *Choanocystis* heliozoan scales. Scale bars = (1, 2) 20 μm ; (3, 4) 10 μm .

common in rocks from 140–122 m (boxes 20–17). Remains of *Paraphysomonas* and *Lepidochromonas* were most abundant between 153–145 m (box 23), and much later at 104–101 m in parts of boxes 13 and 12 (Fig. 4.13). *Raineriophrys* heliozoans were common between 155–150 m (parts of boxes 24 and 23), most abundant at 104–101 m (box 12), and of minor importance in sections corresponding to boxes 20–17 (Fig. 4.5). Remains of testate amoebae plates were found throughout the core, but most abundant in sections below 140 m (boxes 21–26) and again near the termination of the lake phase above 100 m (Fig. 4.2).

Four taxa (*Aulacoseira giraffensis*, *Synura recurvata* Siver and Wolfe, 2005b, *Mallomonas insignis* Penard, 1919, and *Rabdiophrys* sp.) were important components of an extensive portion of the core contained in boxes 20–17 (Fig. 4.4–4.7). *Aulacoseira giraffensis* was abundant and a major component of the lake over a 13 m section, between 138–125 m, and directly corresponding to boxes 20–17 (Fig. 4.6). Remains of *Rabdiophrys* sp. (139–122 m) and *Mallomonas insignis* (141–122 m) largely correlated with those of *A. giraffensis* (Fig. 4.4, 4.5). *Synura recurvata* was also an important species over much of the zone occupied by these three taxa, but conspicuously missing between 125–123 m (Fig. 4.7).

Large sections of the core between 123–105 m (end of box 17 through the beginning of box 13) were dominated by four taxa, *Mallomonas lychenensis*, *M. porifera* Siver and Wolfe, 2005b, *Synura cronbergiae* Siver, 2013, and eunotioid diatoms (Fig. 4.8–4.11). Eunotioid diatoms were common to abundant over an 18 m section from 123–105 m, rare to absent between 105–99 m, and common once again above 99 m (Fig. 4.10). Scales of *M. lychenensis* and *M. porifera* often dominated strata between 121–108 m, and those of *S. cronbergiae* were co-dominant from 113–107 m.

Stratigraphic distributions of two additional taxa are noteworthy. The remains of chrysophyte cysts were abundant throughout the history of the waterbody, often accounting for a significant portion of the microfossil remains, and found in all but one sample (Fig. 4.1). The synurophyte, *Mallomonas bangledashica* (Takahashi and Hayakawa, 1979) Wujek and Timpano, 1984, was common in three different sections (152–150 m [box 23], 140–125 m [boxes 20–17], and near the end of the lake phase between 99–97 m [box 11]).

The percentages of heterotrophic microfossils (Fig. 5.1), based on assignments listed in Table 1, and the ratio of chrysophyte cysts to diatom valves (Fig. 5.2), were calculated for each sample. The percentages of heterotrophic fossils varied widely

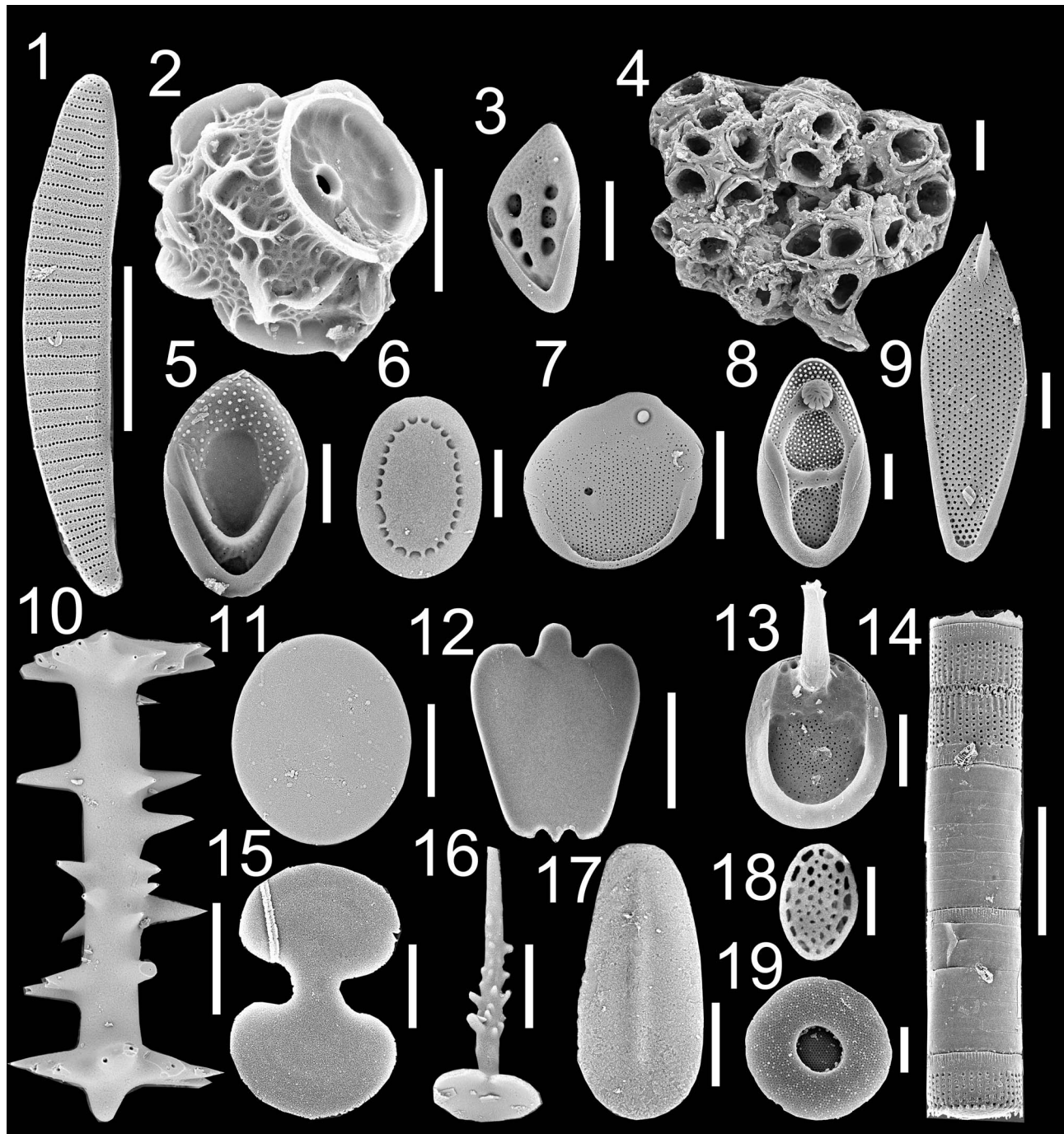


Figure 3. Scanning electron micrographs of microfossil specimens representing 19 of the most important organisms uncovered in the Giraffe Pipe core. (1) Eunoitoid diatom *Actinella*; (2) chrysophyte cyst; (3) scale of *Mallomonas lichenensis*; (4) *Botryococcus* colony; synurophyte scales of (5) *Mallomonas insignis*, (6) *Chryso-sphaerella* Lauterborn, (7) *Mallomonas porifera* Siver and Wolfe, 2005b, (8) *Mallomonas bangladeschica* (Takahashi and Hayakawa, 1979) Wujek and Timpano, 1984, and (9) *Synura cronbergiae* Siver, 2013; (10) sponge spicule; (11, 12) plates of euglyphids; (13) scale of *Synura recurvata* Siver and Wolfe, 2005b; (14) filament of *Aulacoseira giraffensis*; heliozoan scales of (15) *Choanocystis*, (16) *Acanthocystis*, and (17) *Rainieriophrys*; (18) scale of the paraphysomonad, *Lepidochromonas*, and; (19) scale of *Rabdiophrys*. Scale bars are located to the right side of each specimen. Scale bars = (1, 4, 10) 10 μ m; (2, 3, 5, 9, 13, 15–17) 2 μ m; (6, 8, 19) 1 μ m; (7, 11); (12) 5 μ m; (14) 15 μ m; (18) 500 nm 3 μ m.

from 0–88%, with a mean \pm SD of $18 \pm 22\%$. Using a running average, most samples below ~ 120 m contained between 15–22% heterotrophic microfossils (Fig. 5.1). The running averages declined to only 1–2% in samples from 120–109 m, and then increased significantly between 106–99 m, peaking at 103 m with an average of 60% heterotrophs. The cyst to

diatom ratio of the 110 samples that contained diatoms ranged from 0.15–312, with an overall mean of 14. Totals of 82 and 41 of the samples had values >1 and >5 , respectively, signaling the overwhelming importance of chrysophytes. On a broad scale, the cyst to diatom ratio was greatest and reached values well above 20 in core sections below 140 m, between

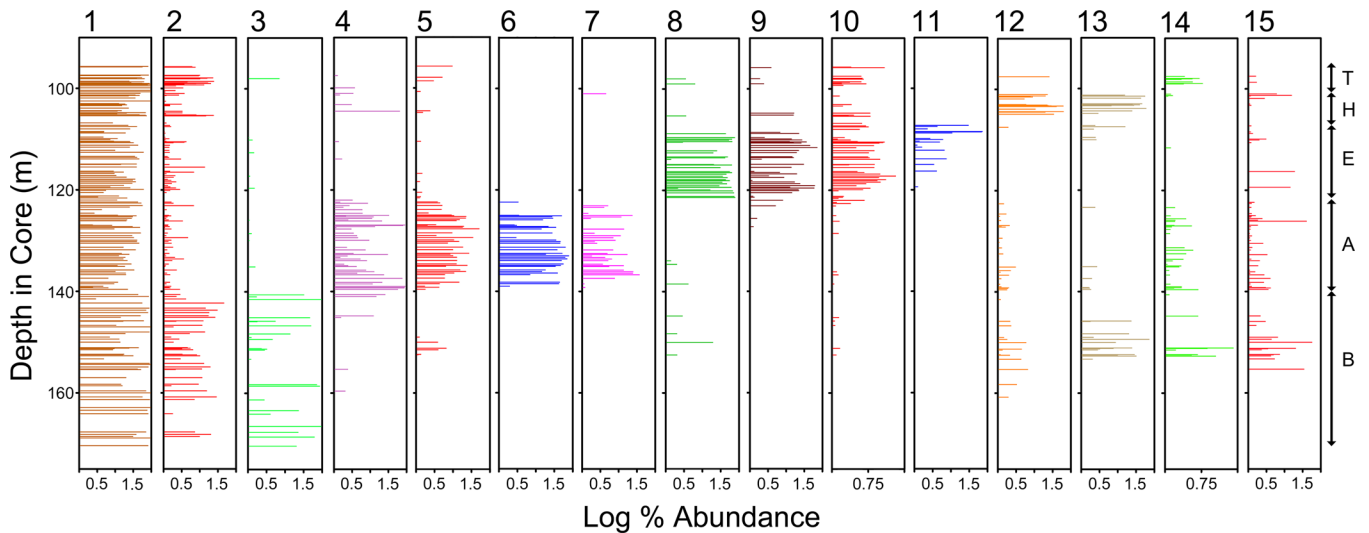


Figure 4. Distribution and abundance of 15 taxa in the Giraffe Pipe core deemed significant for characterizing and distinguishing among the major aquatic zones over the history of the waterbody. (1) Chrysophyte cysts; (2) testate euglyphid plates; (3) *Botryococcus* colonies; (4) *Mallomonas insignis* scales; (5) *Rabdiophrys* scales; (6) *Aulacoseira* valves; (7) *Synura recurvata* scales; (8) *Mallomonas lichenensis* scales; (9) *Mallomonas porifera* scales; (10) eunotioid diatom valves; (11) *Synura cronbergiae* scales; (12) *Raineriophrys* scales; (13) paraphysomonad scales; (14) *Mallomonas bangladeschica* scales; and (15) *Chryso-sphaerella* scales. T = Terminal Lake Zone, H = Heterotrophic Zone, E = Eunotioid Zone, A = *Aulacoseira* Zone, B = *Botryococcus* Zone. Examples of each organism are illustrated in Figure 3.

126–120 m, and with a third peak at ~100 m (Fig. 5.2). Sections with values mostly <5 were found between 135–128 m and 118–112 m, corresponding to peaks in the diatom taxa *A. giraffensis* and eunotioids, respectively.

Shifts in community structure over time.—A multi-step process was used to identify and document the succession of major zones in lake history based on the remains of organisms. Given the large number of samples, abundances of organisms initially were averaged by core box, and the results used in cluster and nMDS ordination analyses (Fig. 6). The cluster with SIMPROF analysis identified six significant groups (Fig. 6.1). Except for samples in box 23, those in boxes 26–24, 22, and 21 formed one cohesive group, referred to herein as the “*Botryococcus* Zone.” A second distinct group comprised samples from boxes 20–17 and is referred to as the “*Aulacoseira* Zone.” Samples in boxes 16–14 formed a third distinct group, referred to as the “Eunotioid Zone.” Samples from boxes 11 and 23 formed a fourth cluster, while those in boxes 12 and 13 were significantly different from the other four groups. With a few exceptions, samples from box 11, which represents the terminal stages of the waterbody and just prior to the transition to a terrestrial environment, had a complement of organisms similar to samples from box 23, which represents a much earlier stage of the lake. Examination of the corresponding nMDS ordination illustrates the degree of similarity between boxes within a cluster, the dissimilarity between clusters, and succession with lake age (Fig. 6.2). The three largest shifts among clusters, correlating with the most significant changes in community structure, were between the *Botryococcus* and *Aulacoseira* zones, the *Aulacoseira* and Eunotioid zones, and the Eunotioid and younger lake zones.

Although initially averaging all samples by box provided an excellent preliminary means to identify major lake zones, a cluster with SIMPROF analysis using all 175 samples was

used next to finalize sample assignments into zones, and to identify more precise transition points between zones (Fig. 7). Zone assignments for the majority of samples did not change with the following four exceptions: (1) samples in the lower part of box 20 were reassigned from the *Aulacoseira* Zone to the *Botryococcus* Zone; (2) samples in the lower channels of box 13 clustered with the Eunotioid Zone; (3) samples in the top portion of box 13 and most of box 12 grouped together, forming the “Heterotrophic Zone;” and (4) samples in the upper portion of box 12 and those in box 11 clustered to form a fifth major zone, the “Terminal Lake Zone.”

SIMPLER analyses were used to determine which organisms were most important for distinguishing among all samples regardless of zone assignment, and among the five identified lake zones. Based on an initial SIMPLER analysis, *Mallomonas porifera*, *Synura cronbergiae*, *Scutiglypha* testates, *Rabdiophrys* sp., and *Acanthocystis* heliozoans were the most important taxa distinguishing among all samples ($r=0.90$). The next most important taxa included *Botryococcus*, cysts <10 μm , *Raineriophrys* heliozoans, the *Mallomonas lichenensis* species complex, and eunotioid diatoms.

SIMPLER analyses were then used to identify the most important organisms associated with transitions between lake zones, which in turn could be used to infer changes in environmental conditions associated with each zone (Tables 2–5). Eleven taxa accounted for 72.4% of the difference between the *Botryococcus* and *Aulacoseira* zones (Table 2), and samples from both zones were well separated in the nMDS ordination (Fig. 8). This suite of organisms included those that dominated the *Aulacoseira* Zone (*A. giraffensis*, *Rabdiophrys* sp., *Mallomonas insignis*, and *Synura recurvata*) and those that dominated the *Botryococcus* Zone (testate amoebae and *Botryococcus*). The transition between the *Aulacoseira* and Eunotioid zones (Fig. 8) was characterized by the virtual disappearance of taxa that dominated in the *Aulacoseira* Zone, and replacement with

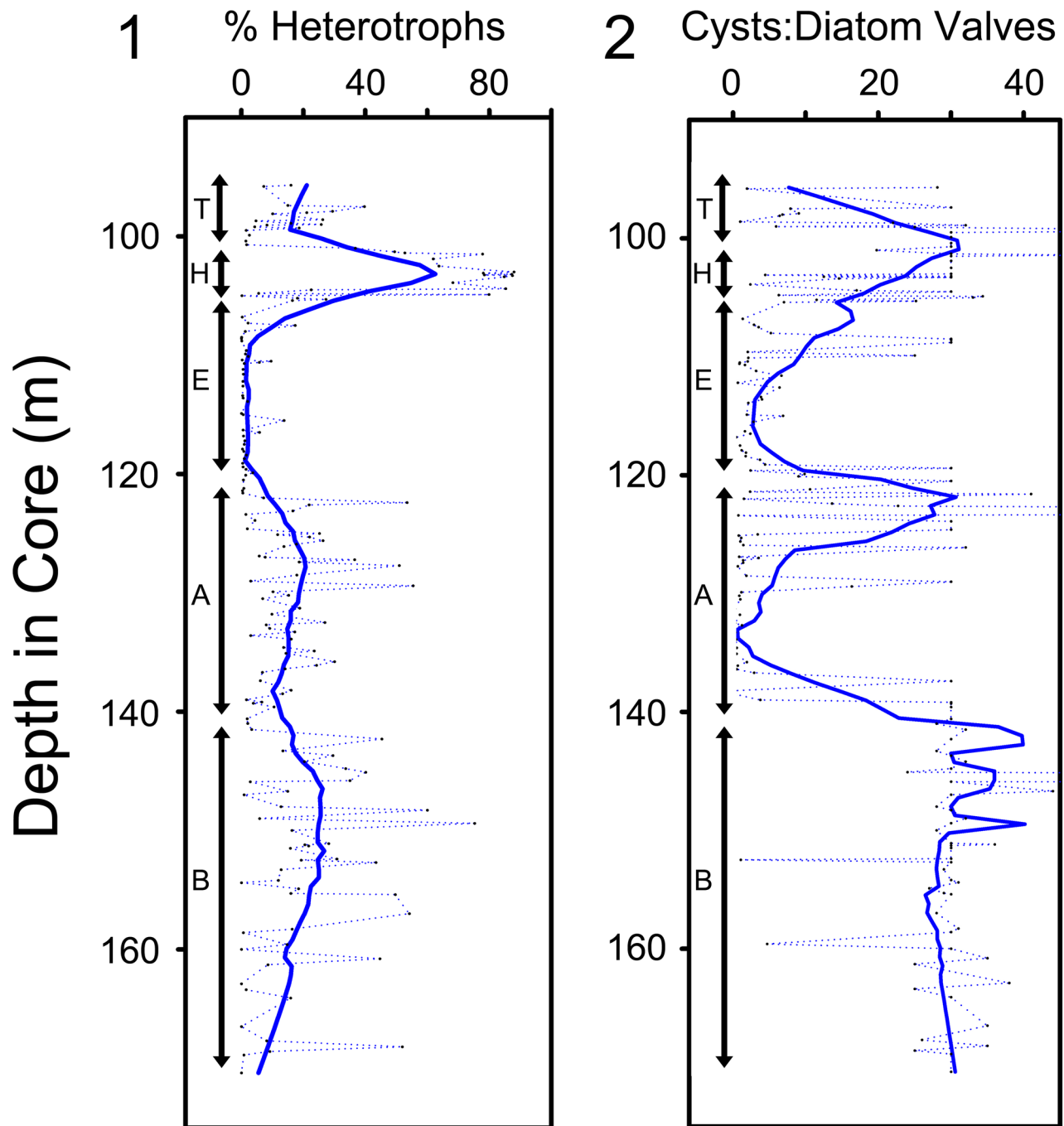


Figure 5. Results of (1) the percentage of microfossils representing heterotrophic organisms, and (2) the ratio of chrysophyte cysts to diatom valves in the Giraffe Pipe core. The solid line represents a running average. T = Terminal Lake Zone, H = Heterotrophic Zone, E = Eunotioid Zone, A = *Aulacoseira* Zone, B = *Botryococcus* Zone.

Mallomonas lychenensis, *M. porifera*, *Synura cronbergiae*, and a large rise in eunotioid diatoms (Table 3). This suite of organisms accounted for 71% of the difference between the two zones. The transition from the Eunotioid Zone to the Heterotrophic Zone (Fig. 9) occurred suddenly and was marked by the decline and disappearance of almost all autotrophic protists, and replacement with large numbers of heliozoans and paraphysomonads (Table 4). The final transition from the Heterotrophic Zone to the Terminal Lake Zone was characterized by significant declines in paraphysomonads and heliozoans, coupled with

increases in *Mallomonas asmundiae* (Wujek and Van Der Veer, 1976) Nicholls, 1982, *Scutiglypha* testates, cysts, sponge spicules, and the reemergence of eunotioid diatoms (Table 5).

Core lithology in relationship to lake zones.—Although a detailed analysis of the core material was beyond the scope of this study, superficial characteristics of the core were found to correlate nicely with the five zones identified using the microfossil remains (Fig. 10). A large portion of the core associated with the *Botryococcus* Zone consisted of crumbled

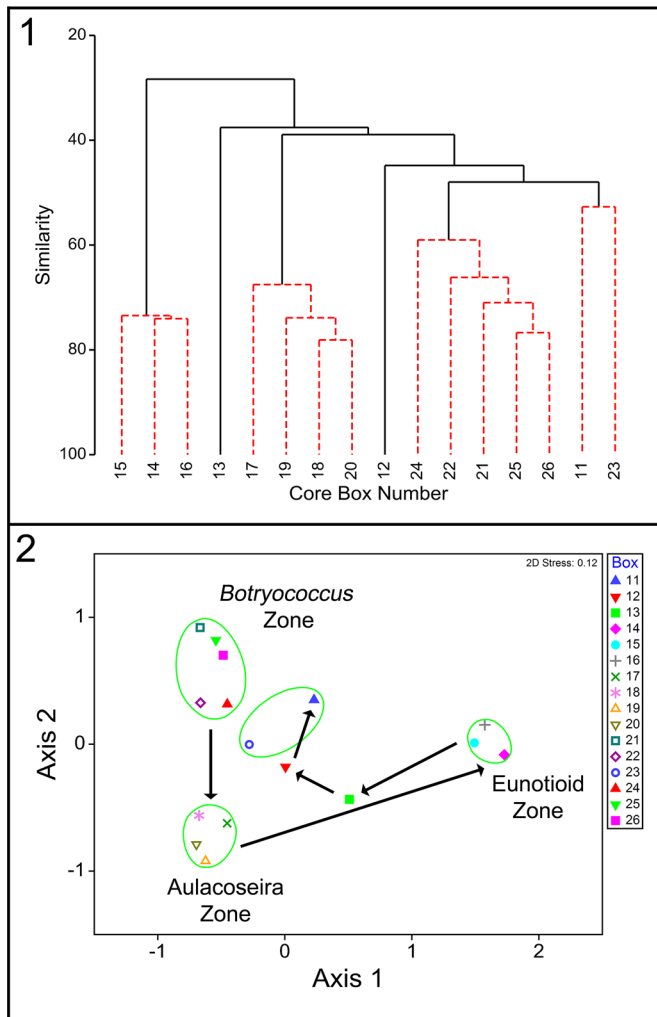


Figure 6. Results of (1) cluster and (2) non-metric multidimensional scaled ordination (nMDS) analyses of 175 samples within the lacustrine phase of the Giraffe Pipe core based on abundances of 58 taxa and averaged by core box. (1) Cluster analysis: four significant clusters (denoted by dashed lines) were detected based a SIMPROF test. Samples in boxes 12 and 13 were significantly different from all others. (2) nMDS Ordination: the four significant clusters identified with the SIMPROF test are depicted, and the set of arrows traces a time sequence from the inception to the end of the lacustrine phase. See text for details.

mudstone and shale fragments, often inundated with siliceous opal-A deposits (Fig. 10.1–10.3). The transition between the *Botryococcus* and *Aulacoseira* zones was distinct and marked by a change to massive light-brown siltstones starting in box 20 (Fig. 10.4), which continued through boxes 19 (Fig. 10.5) and 18 (Fig. 10.6). The lower portion of the Eunotioid Zone consisted of laminated organic mudstones (Fig. 10.7). The mudstones become increasingly dark brown to black in color and massive towards the upper section of the zone (Fig. 10.8), before transitioning abruptly to the Heterotrophic Zone (Fig. 10.9). The massive light brown siltstone characterizing the Heterotrophic Zone continued through the lower channel in box 12 (Fig. 10.10), and the termination of this zone is marked by the siltstones becoming infiltrated with opal-A deposits (Fig. 10.11). The Terminal Lake Zone begins in the upper channel of box 12, which is characterized once again

with dark organic mudstones (Fig. 10.12) that remain throughout box 11 (Fig. 10.13) until the end of the lake phase.

Discussion

The Giraffe Pipe locality represents one of the most remarkable freshwater fossil sites known from the Eocene, and arguably the most valuable one situated near the Arctic Circle. The preservation quality and sheer number of fossil specimens, representing many eukaryotic lineages, are outstanding. The excellent quality of the siliceous microfossils in particular is likely related to minimal dissolution regulated, in part, by elevated concentrations of dissolved silica in the Giraffe Pipe waterbody (Wolfe et al., 2006). The fossil locality has provided and will continue to provide information on the evolutionary histories of multiple lineages (e.g., Barber et al., 2013; Siver and Skogstad, 2022), and yield insights for understanding potential effects of future warming on freshwater habitats across northern latitude regions (Siver and Wolfe, 2009; Pisera et al., 2013). Unlike paleolimnological investigations based on recent lake sediments, the siliceous components comprising the cell coverings on many unicellular protists found within the rocks at the Giraffe Pipe locality are often observed intact, yielding valuable cell-level details (Siver, 2018, 2020). Even more remarkable, Wolfe et al. (2006) demonstrated organelle-level resolution, including ultrastructural details of diatom plastids from Giraffe Pipe locality specimens. Such cell and subcellular level information as preserved in Giraffe Pipe rocks offers an element of evolutionary history, in addition to species diversity information, not known from other similar-aged fossil localities.

Despite hundreds of previous paleontological investigations, including many focused on diatoms, the Giraffe Pipe locality was the first fossil site where remains of scaled chrysophytes older than the Holocene were discovered (Siver and Wolfe, 2005a). Even more outstanding were the concentrations and diversity of chrysophyte microfossils entombed within the Giraffe Pipe crater. Chrysophyte scales and cysts accounted for 37% and 35% of all specimens uncovered in the study, and collectively they comprised >50% in 136 of the 175 samples analyzed. The overall importance of the chrysophytes can be implied further by inspecting the ratio of specimens in this lineage to those in the Bacillariophyceae (diatoms). The ratio of cysts to diatom valves has been widely used as a tool in paleolimnological research, especially with respect to understanding shifts in trophic conditions (Smol, 1985; Douglas and Smol, 1995; Li et al., 2010) and effects of climate (Stager et al., 2021). Typically, values close to 1 indicate more oligotrophic conditions and an elevated importance of chrysophytes, and values <1 imply more eutrophic habitats (in most studies, values of this ratio are <1). The values found throughout most of the Giraffe Pipe core are significantly higher than those reported in modern waterbodies, with a mean ratio of 13.6, further emphasizing the dominance of the chrysophyte lineage at this locality and during this geologic time period. Foissner (2006) defines a biodiversity “hotspot” as a region that contains a high percentage of the total species known globally (i.e., a high local-to-global ratio). Although an estimate of the number of chrysophyte species that existed worldwide during the Eocene is not known, given the high diversity found in the

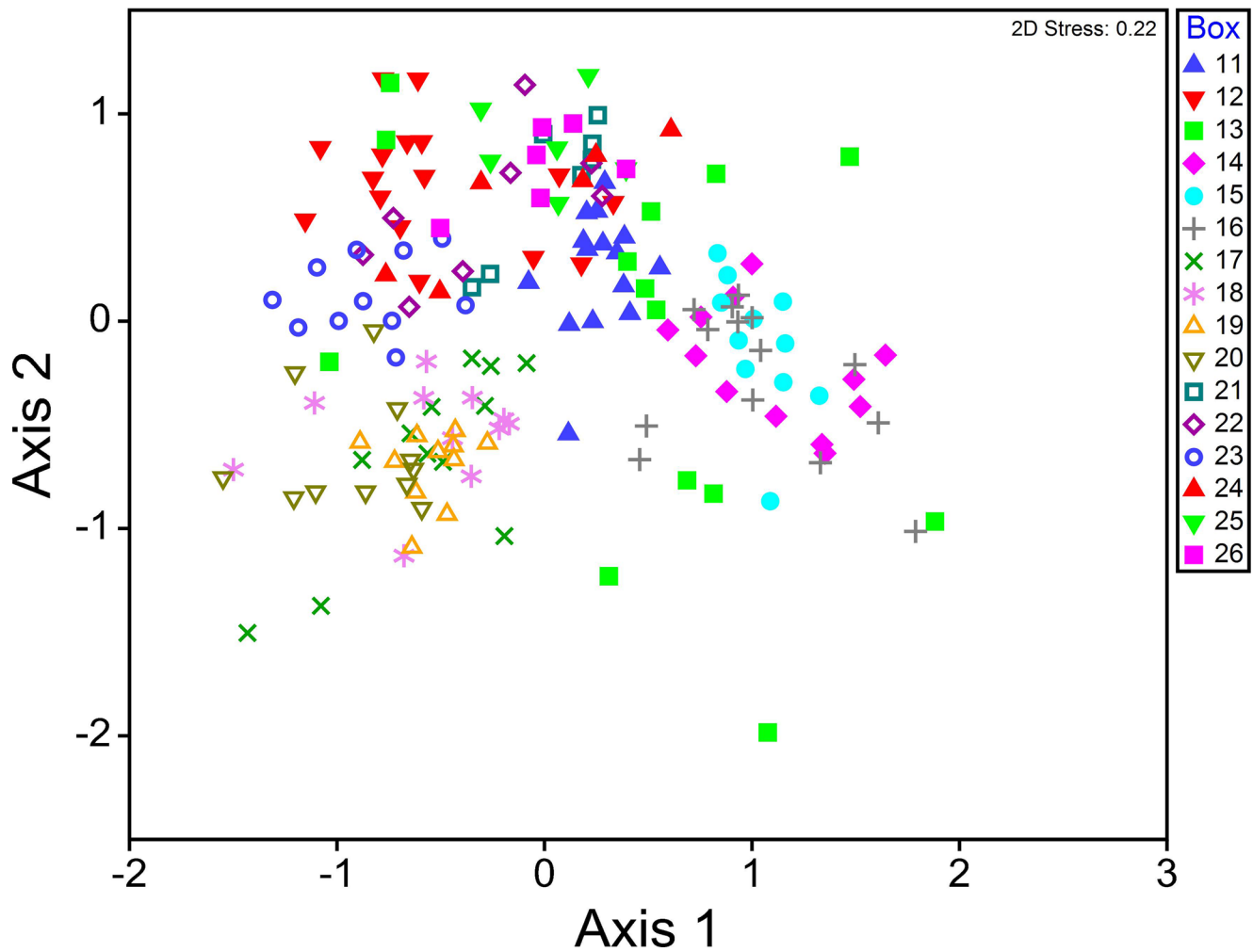


Figure 7. Results of non-metric multidimensional scaled ordination (nMDS) analyses of 175 samples distributed in 16 core boxes (11–26) within the lacustrine phase of the Giraffe Pipe core based on abundances of 58 taxa. Samples within a given core box, with the exception of those in box 13, cluster close together.

Giraffe Pipe crater relative to the vast majority of modern localities examined worldwide, it could be described as a “paleo-hotspot” with respect to chrysophyte diversity.

A closer look at modern sites that harbor high diversities of chrysophytes may yield insight as to the conditions that

supported such a haven for growth of chrysophytes in the Giraffe Pipe waterbody. In a broad sense, based on a thorough literature search, Siver (1995, 2015) summarized the habitats that support especially high concentrations of chrysophytes as ones that are typically acidic, low in dissolved salts, alkalinity, and nutrient

Table 2. Results of a SIMPER analysis identifying the organisms that contribute the most to the transition between the *Botryococcus* and *Aulacoseira* Zones in the Eocene waterbody from the Giraffe Pipe locality. Abundance numbers represent mean $\log_e(X + 1)$ values. The number in parentheses under the % contribution column represents a cumulative % contribution.

Taxon	Mean Abundance		Average Dissimilarity	Diss/SD	% Contribution
	<i>Aulacoseira</i> Zone	<i>Botryococcus</i> Zone			
Centric diatoms ¹	2.33	0.08	8.25	1.32	11.5
<i>Rabdiophrys</i> sp.	2.06	0.0	7.29	2.01	10.2
<i>Mallomonas insignis</i>	2.04	0.7	6.77	1.23	9.4
Cysts $\leq 10 \mu\text{m}$	2.8	3.8	4.86	1.19	6.8
<i>Botryococcus</i> sp.	0.02	1.33	4.73	0.75	6.6
<i>Synura recurvata</i>	1.19	0.0	4.04	1.05	5.6
Testates <i>Scutiglypha</i> spp.	0.18	1.26	3.94	1.28	5.5
Testates <i>Euglypha</i> spp.	0.19	1.12	3.5	1.41	4.9
Heliozoans A	0.69	0.63	3.15	1.00	4.4
Heliozoans B	0.38	0.64	2.76	0.75	3.8
<i>Synura nygaardii</i>	0.74	0.0	2.67	0.54	3.7 (72.4%)

¹*Aulacoseira giraffensis* accounted for 96% of the Centric diatom category.

Table 3. Results of a SIMPER analysis identifying the organisms that contribute the most to the transition between the *Aulacoseira* and *Eunotia* Zones in the Eocene waterbody from the Giraffe Pipe locality. Abundance numbers represent mean $\log_e(X + 1)$ values. The number in parentheses under the % contribution column represents a cumulative % contribution.

Taxon	Mean Abundance		Average Dissimilarity	Diss/SD	% Contribution
	<i>Aulacoseira</i> Zone	<i>Eunotia</i> Zone			
<i>Mallomonas lychenensis</i>	0.04	2.84	9.49	1.62	12.1
Centric diatoms ¹	2.33	0.04	7.63	1.36	9.7
<i>Mallomonas porifera</i>	0.05	2.31	7.42	1.66	9.4
<i>Mallomonas insignis</i>	2.04	0.05	6.68	1.33	8.5
<i>Rabdiophrys</i> sp.	2.06	0.05	6.57	2.07	8.3
Eunotioid diatoms ²	0.08	1.96	6.15	1.70	7.8
<i>Synura recurvata</i>	1.19	0.0	3.73	1.06	4.7
<i>Synura cronbergiae</i>	0.0	0.39	3.14	1.17	4.0
<i>Synura nygaardii</i>	0.74	0.03	2.48	0.56	3.2
<i>Acanthocystis</i> heliozoans	0.69	0.12	2.22	0.87	2.8 (71%)

¹*Aulacoseira giraffensis* accounted for 96% of the Centric diatom category.

²Includes multiple species of *Eunotia* and *Actinella*.

content, and with moderate amounts of dissolved humic substances. These waterbodies also tended to be small, shallow ponds or wetlands, often situated in forested areas (Cronberg and Kristiansen, 1980; Eloranta, 1989; Kristiansen, 2005). Based on the organisms uncovered in our study, and discussed below, the Giraffe Pipe waterbody is inferred to have been shallow over extensive periods of time, with varying degrees of acidity, humic content, and nutrient levels. This suite of conditions is similar to those found in habitats supporting high diversity levels today (Siver, 2015), and we know that the surrounding landscape consisted of a *Metasequoia*-dominated forest (Doria et al., 2011; Wolfe et al., 2017).

Another potential factor contributing to the high diversity and growth of chrysophytes in the Giraffe Pipe waterbody is the fact that these organisms lack carbon-concentrating mechanisms (CCMs; Bhatti and Colman, 2005; Raven et al., 2005, 2012), and therefore rely on diffusion of CO₂ into the cell and to the plastid for photosynthesis, which is a process modulated by ambient pCO₂ levels (Wolfe and Siver, 2013). Atmospheric concentrations of CO₂ during the early Eocene were significantly higher than present day levels (Zachos et al., 2008; Pagani et al., 2014), and median concentrations specific for the Giraffe Pipe locality were close to double those of preindustrial levels (Doria et al., 2011; Wolfe et al., 2017). High atmospheric CO₂ concentrations, coupled with acidic pH and elevated dissolved organic matter, likely would have resulted in supersaturated

levels of CO₂ in the Giraffe Pipe water column (Pace and Cole, 2002; Kritzbeg and Ekström, 2012), potentially favoring algal taxa that lack CCMs. A similar mechanism was hypothesized to explain recent increases in chrysophyte algae in boreal and Arctic lakes as a result of climate change (Wolfe and Perren, 2001; Wolfe and Siver, 2013).

Earth experienced greenhouse conditions during the early to late Eocene, with significantly higher mean annual temperatures (MAT), lack of permanent polar ice, and winter conditions above freezing (Zachos et al., 2008; Pagani et al., 2014; Barral et al., 2017; Westerhold et al., 2020). In addition, polar amplification resulted in even higher MAT values in northern regions relative to today. Wolfe et al. (2017) reported MATs >17°C warmer than present, and mean annual precipitation (MAP) >4× present conditions for the Giraffe Pipe locality, supporting pollen data that indicate a warm, humid forest environment. In addition, the Giraffe Pipe locality contains microfossil remains of multiple organisms that today are restricted to tropical-subtropical regions. These include lineages of synurophytes, diatoms (Siver and Wolfe, 2009), sponges (Pisera et al., 2013, 2016), and palm phytoliths, and further indicate that the waterbody experienced a warm subtropical-like climate. Our findings fully support these previous works, and further imply that aquatic organisms presently restricted to lower latitudes could grow and thrive in Arctic habitats under future warming scenarios.

Table 4. Results of a SIMPER analysis identifying the organisms that contribute the most to the transition between the Eunotioid and Heterotrophic zones in the Eocene waterbody from the Giraffe Pipe locality. Abundance numbers represent mean $\log_e(X + 1)$ values. The number in parentheses under the % contribution column represents a cumulative % contribution.

Taxon	Mean Abundance		Average Dissimilarity	Diss/SD	% Contribution
	Heterotrophic Zone	<i>Eunotia</i> Zone			
<i>Mallomonas lychenensis</i>	0.0	2.84	10.67	1.56	13.83
<i>Rainieriophrys</i> heliozoans	2.61	0.0	9.30	1.91	12.05
<i>Mallomonas porifera</i>	0.0	2.31	8.35	1.63	10.82
Paraphysomonads	2.3	0.05	8.12	1.47	10.52
Eunotioid diatoms ¹	0.14	1.96	6.72	1.63	8.70
<i>Acanthocystis</i> heliozoans	1.78	0.12	6.08	1.13	7.88
<i>Choanocystis</i> heliozoans	1.13	0.06	3.83	0.98	4.98
Cysts ≤10 μm	3.19	2.84	3.84	1.04	4.51 (73%)

¹Includes multiple species of *Eunotia* and *Actinella*.

Table 5. Results of a SIMPER analysis identifying the organisms that contribute the most to the transition between the Heterotrophic and Terminal Lake zones in the Eocene waterbody from the Giraffe Pipe locality. Abundance numbers represent mean $\log_e(X + 1)$ values. The number in parentheses under the % contribution column represents a cumulative % contribution.

Taxon	Mean Abundance		Average Dissimilarity	Diss/SD	% Contribution
	Terminal Lake Zone	Heterotrophic Zone			
Paraphysomonads	0.0	2.18	7.39	1.27	10.9
<i>Raineriophrys</i> heliozoans	0.22	2.11	6.98	1.34	10.29
<i>Mallomonas asmundiae</i>	1.69	0.02	5.63	1.18	8.29
<i>Scutyglypha</i> testates	1.71	0.15	5.53	1.91	8.15
<i>Acanthocystis</i> heliozoans	0.12	1.65	5.39	1.07	7.94
Eunotioid diatoms ¹	1.29	0.15	4.03	1.36	5.95
<i>Choanocystis</i> heliozoans	0.0	1.2	3.93	1.01	5.79
Cysts >10 μ m	1.04	0.44	3.75	0.97	5.53
Sponge spicules	1.06	0.12	3.35	1.55	4.93
Cysts <10 μ m	4.01	3.4	3.17	1.38	4.68 (72.5%)

¹Includes multiple species of *Eunotia* and *Actinella*.

Our initial hypothesis was that once the Giraffe Pipe crater formed, it filled with water forming a deep lake, then slowly infilled with sediment over thousands of years, becoming a shallow lake, eventually a wetland, and finally a terrestrial landscape. However, based on our findings it is clear that for extended periods of time the aquatic habitat contained within the crater was relatively shallow, with changing physical and chemical conditions, and varying water depths. We identified five major zones based on the remains of organisms, most of which were stable for extended periods of time. The transitions between successive zones mostly occurred relatively rapidly, over short time periods, indicating significant shifts in physical and chemical conditions. The transitions from the *Botryococcus* Zone to the *Aulacoseira* Zone, and between the Eunotioid Zone and Heterotrophic Zone, occurred suddenly, as indicated by rapid shifts in the complements of organisms, coupled with lithographic changes observed over a few centimeters of core material. The transitions between the *Aulacoseira* Zone and Eunotioid Zone and from the Heterotrophic Zone to the Terminal Lake Zone were more gradual, but in each case eventually resulted in a widely different complement of organisms and distinctive changes in characteristics of the associated rocks.

Several lines of evidence support the hypothesis that the initial waterbody found in the crater, and represented by the *Botryococcus* Zone, was shallow, slightly acidic, and with low to moderate nutrient concentrations. Euglyphid testate amoebae plates accounted for ~30% of the microfossils in this zone, which is similar to their abundance in the Terminal Lake Zone, but significantly higher than periods in between. Testate amoebae are most common and abundant in shallow lakes and ponds, wetlands, peatlands, and bogs, as well as in wet organic-rich soils and moss beds (Ogden and Hedley, 1980; Escobar et al., 2008; Mitchell et al., 2008; Amesbury et al., 2018; Siver et al., 2020). In addition, water depth and pH often are reported as the most important variables controlling diversity and abundance of testate amoebae in freshwater habitats (Mitchell et al., 1999; Booth, 2002; Patterson et al., 2012; McKeown et al., 2019; Tsyganov et al., 2019; Siver et al., 2020). In a study specifically targeting euglyphid testates, Siver et al. (2020) reported the highest concentrations in shallow habitats <1 m in depth that were moderately acidic. Based on the models developed by Siver et al. (2020) relating euglyphid

abundance to water depth and pH, depths of the Giraffe Pipe waterbody during the *Botryococcus* Zone were ~1 m, and pH values between 5–6. Although diatoms are rare in the *Botryococcus* Zone, those present were attached forms and this zone lacked planktic diatom species, supporting the hypothesis that the waterbody was shallow. *Botryococcus* is found in the fossil record since the Precambrian and its morphology remained virtually unchanged throughout the Phanerozoic (Guy-Ohlson, 1992). *Botryococcus*, found in both the plankton and on surface sediments, is common in lakes, ponds, and bogs, and has been characterized as an “early colonizer,” and indicator of oligotrophic conditions that competes best in shallow and calm conditions (Guy-Ohlson, 1992; Tyson, 1995; Smittenberg et al., 2005). Smittenberg et al. (2005) further proposed that disappearance of *Botryococcus* in the paleo-records of aquatic habitats was an indicator of increased eutrophication.

The continued presence of *Botryococcus* throughout the early period of the Giraffe Pipe waterbody further supports the hypothesis that it was a shallow and stable environment, and its disappearance possibly resulted from deepening of the waterbody coupled with an increase in nutrients. This point in time marked the transition to the *Aulacoseira* Zone, which occurred abruptly in the ontogeny of the Giraffe Pipe waterbody. The disappearance of *Botryococcus*, along with a seven-fold decline in testate euglyphids, was coupled with the sudden appearances of *Aulacoseira giraffensis* and *Rabdiophrys* sp., and a five-fold increase in synurophytes. The transition is further marked with an increase in synurophyte diversity from six species found in the *Botryococcus* Zone to 18 species in the *Aulacoseira* Zone, dominated by a three-fold increase in *Mallomonas insignis* and establishment of substantial populations of the motile colonial taxa, *Synura recurvata* and *S. nygaardii* (Petersen and Hansen, 1956) Kristiansen, 1997.

Multiple lines of evidence support deepening of the waterbody concurrent with the *Aulacoseira* Zone, from a shallow wetland to a moderately deep pond. First, species of *Aulacoseira* that form filaments consisting of numerous cells held together with linkage spines, as is the case for *A. giraffensis*, most often inhabit the planktic zone and are maintained in the water column through wind-induced mixing (Edlund et al., 1996; Siver and Kling, 1997; Houk and Klee, 2007; Jewson et al., 2008; Boeff et al., 2016). Second, the significant increase in synurophyte diversity,

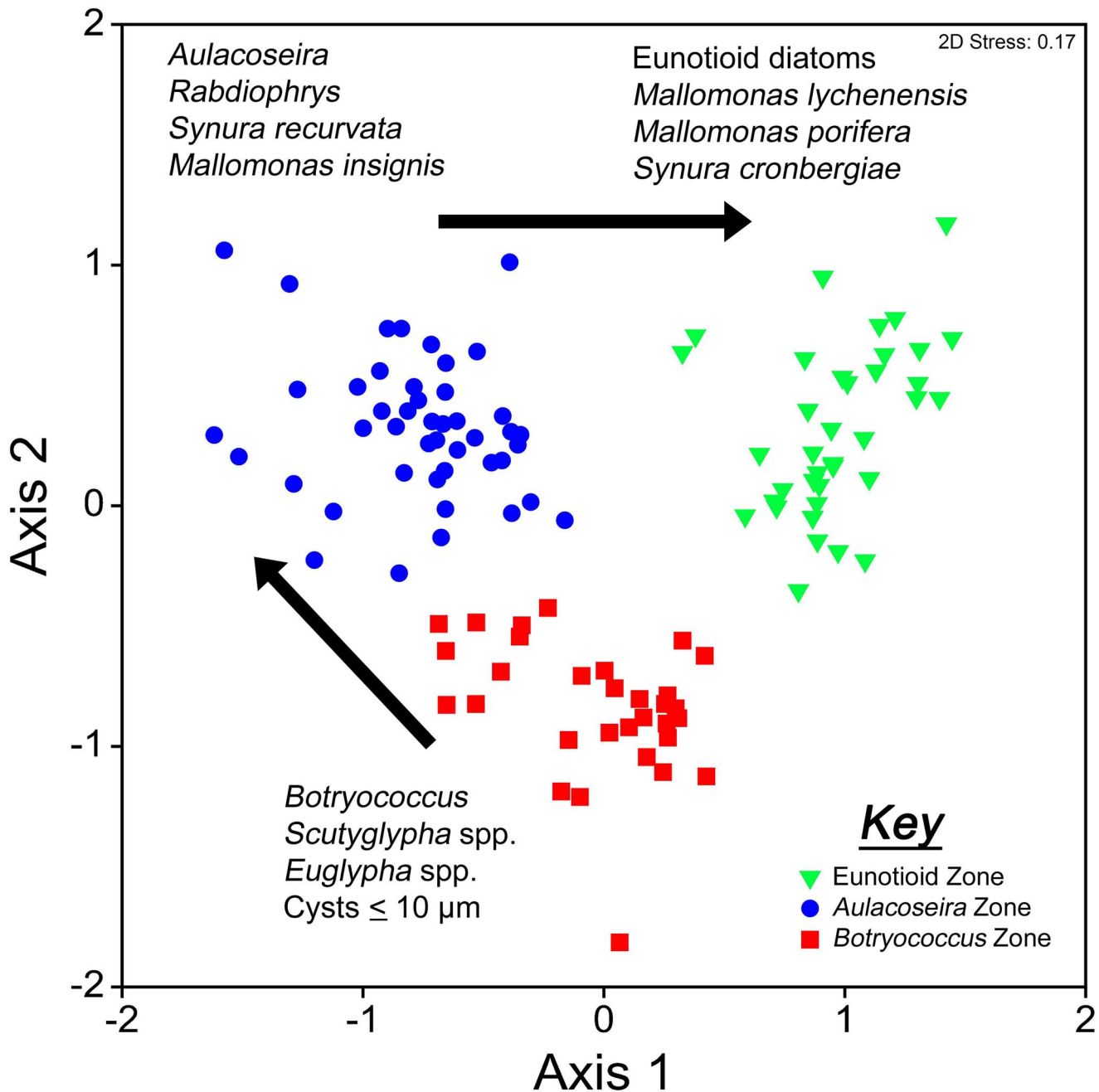


Figure 8. Results of non-metric multidimensional scaled ordination (nMDS) analyses of the samples representing three consecutive zones within the lacustrine waterbody, the *Botryococcus* Zone (red), the *Aulacoseira* Zone (blue), and the Eunotioid Zone (green). The most important organisms characterizing each zone are given and the arrows indicate a time sequence among the three zones.

especially *Synura* species, is consistent with a small lake or pond with a modest planktic zone (Siver, 1995, 2015). Interestingly, Siver and Lott (2012) reported *S. uvella* Ehrenberg, 1834, emended Korshikov, 1929, the closest modern congener of *S. recurvata*, and *M. insignis* growing together in small, mesotrophic, and circumneutral ponds with water depths of 3–5 m. Third, declines in euglyphid testates further signals an increase in water depth (Siver et al., 2020). The decline in *Botryococcus*, coupled with a thriving chrysophyte community and high abundances of *Aulacoseira*, also imply moderate nutrient levels (Smit-tenberg et al., 2005; Nicholls and Wujek, 2015; Siver, 2015).

Siemensma (1981) reported finding the modern species *Rabdiophrys monopora* (Thomsen, 1978) Roijackers and Siemensma, 1988, in eutrophic waterbodies, lending further support that the *Aulacoseira* Zone witnessed an increase in nutrients. However, because the ecological conditions that enhance growth of *Rabdiophrys* species are otherwise unknown (Siver and Skogstad, 2022), future study of this heterotrophic protist will only enhance our reconstruction of the Giraffe Pipe waterbody and other waterbodies harboring this protist.

The transition from the *Aulacoseira* Zone to the Eunotioid Zone was marked by a significant shift in the complement of fossil

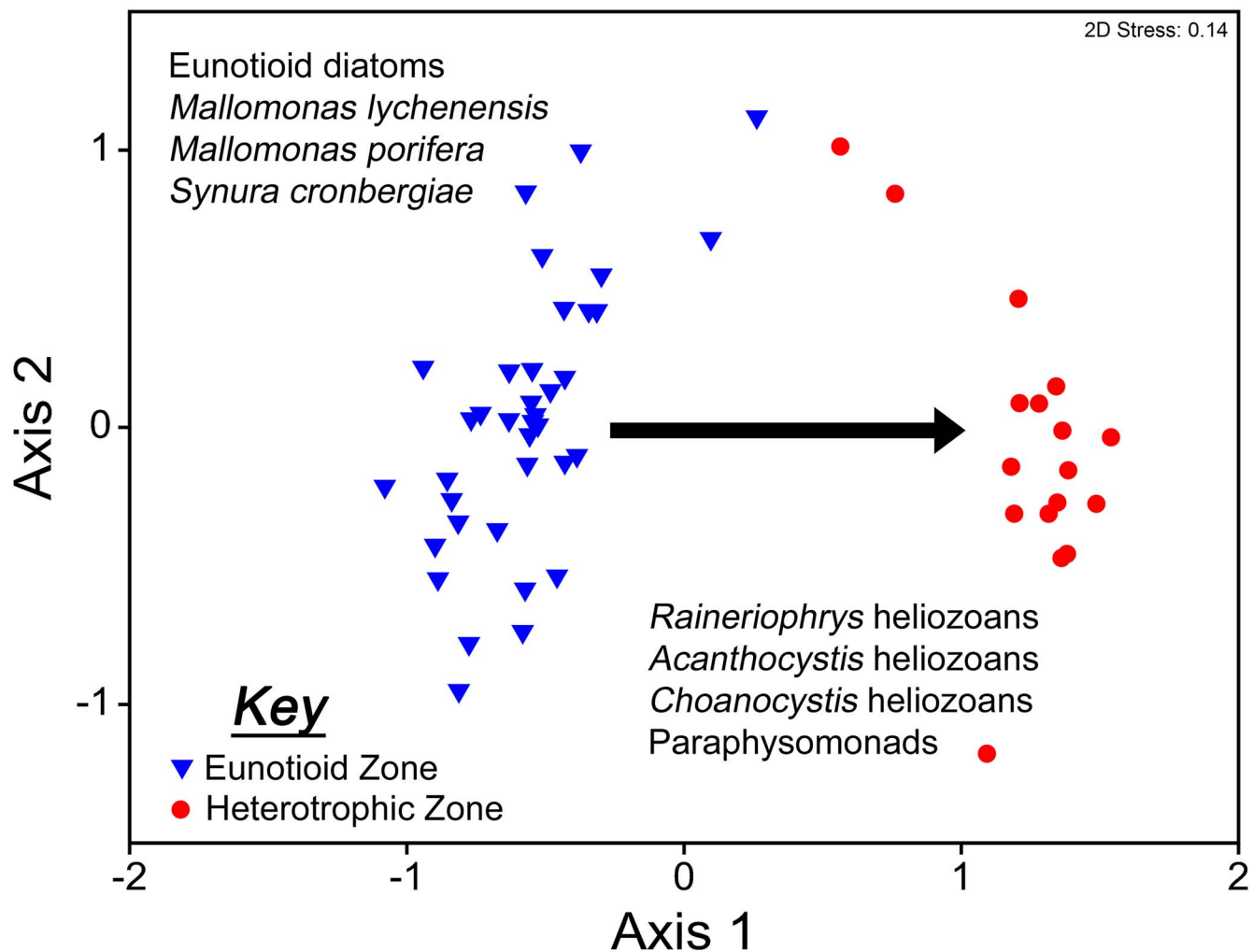


Figure 9. Results of non-metric multidimensional scaled ordination (nMDS) analyses of the samples representing two consecutive zones within the lacustrine waterbody, the Eunotioid Zone (blue), and the Heterotrophic Zone (red). The most important organisms characterizing each zone are given.

remains, as well as in core lithology, both supporting a hypothesis where the waterbody continued to acidify and increase in dissolved humic material. The once dominant diatom, *Aulacoseira giraffensis*, was replaced by numerous species of the genera *Eunotia*, *Actinella*, and *Oxyneis*, all characteristic of shallow, acidic, and humic-stained waterbodies (Round et al., 1990; Metzeltin and Lange-Bertalot, 1998, 2007; Camburn and Charles, 2000; Siver et al., 2005; Melo et al., 2010; Siver and Hamilton, 2011). Abundances and species diversity of synurophytes, already substantial in the *Aulacoseira* Zone, were even greater in the Eunotioid Zone, increasing by 31% and 67%, respectively. In fact, >30 synurophyte species have been uncovered in the Eunotioid Zone strata and their scales accounted for 55% of all microfossils, further supporting the concept that the Giraffe Pipe locality represents a paleo-hotspot for synurophytes.

The pH consistently has been shown to be one of the most important variables controlling synurophyte species (Siver, 1989, 2015; Siver and Hamer, 1989; Cumming et al., 1992, 1994). Siver and Hamer (1989) reported the highest numbers of species (mean = 9) in samples between pH 5.5–6, with slightly fewer between pH 4.5–5.5, and considerably fewer above pH 7.5–8. Based on these findings, the high diversity of

synurophytes, coupled with the abundance of all chrysophytes (scales and cysts = 77% of fossil specimens), is consistent with an acidic waterbody.

The dominant diatoms found in the Eunotioid Zone further support an acidic waterbody with elevated dissolved humic matter and low nutrients. Species of *Eunotia* overwhelmingly inhabit waterbodies with low pH, and this taxon is one of the most acidophilic diatom genera known (Camburn and Charles, 2000; Gaiser and Johansen, 2000; Siver and Hamilton, 2011). In a study of a diverse suite of lakes and ponds on Cape Cod (Massachusetts, USA), Siver et al. (2005) reported 17 of 18 *Eunotia* species with average weighted mean pH (AWMpH) values ranging between 4.9–5.8. Similar findings were reported by Camburn and Charles (2000) for the Adirondack Mountain region, and by Siver and Hamilton (2011) for ponds along the Atlantic Coastal Plain, where 37 of 40 species and 31 of 32 species had AWMpH scores below 5.9, respectively. Gaiser and Johansen (2000) and Metzeltin and Lange-Bertalot (2007) found *Eunotia* dominating in numerous acidic, dystrophic, and nutrient-poor waterbodies.

Like *Eunotia*, *Actinella* and *Oxyneis* are also largely restricted to very acidic and mostly dystrophic habitats (Round

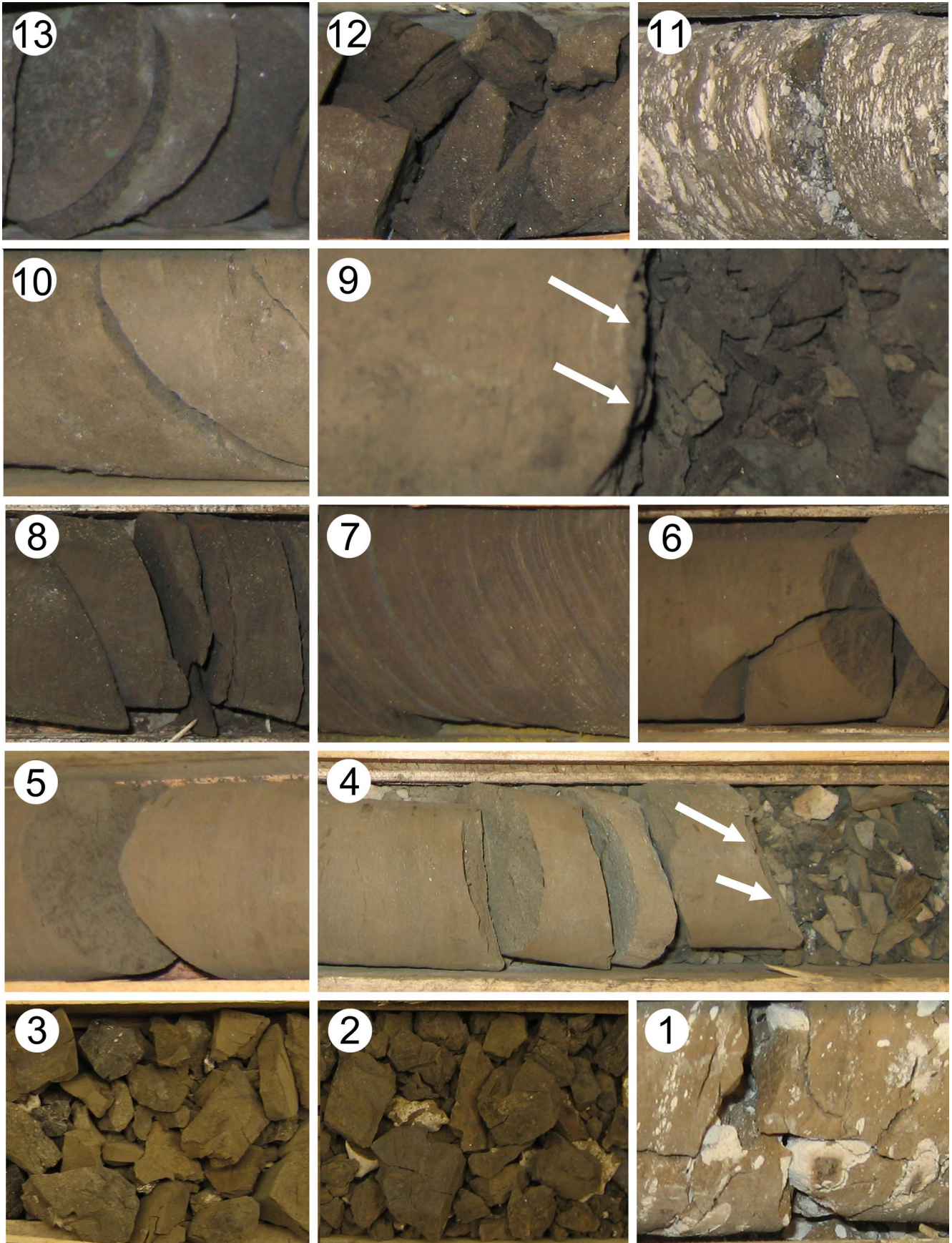


Figure 10. Representative images of the Giraffe Pipe core relative to the major shifts in community structure. Images are arranged from (1) near the onset of the lacustrine phase at the bottom of the core to (13) close to the termination of the lake phase and just before the transition to a terrestrial environment. (1–3) Three sections within the *Botryococcus* Zone from boxes 24, 21, and 20, respectively. This section of the core consists largely of crumbled rock fragments, some of which contain deposits of (1) siliceous nodules, and most of which are (2, 3) medium-brown colored organic mudstones. (4) Section of the core within box 20 showing the distinct transition from the *Botryococcus* Zone to the *Aulacoseira* Zone (arrows), the latter of which consists of massive light-brown siltstones. (5, 6) Continuation of the *Aulacoseira* Zone in boxes (5) 19 and (6) 18. (7) The lower portion of the Eunotioid Zone, mostly in box 16 and part of box 15, depicted by mudstones containing distinct laminations. (8, 9) The upper component of the Eunotioid Zone, which extends from (8) the middle of box 15 to (9) the upper channel of box 13, is characterized by dark-brown to black organic mudstones. The image represented in (9) depicts the distinct transition zone (arrows) marking the end of the Eunotioid Zone and the beginning of the Heterotrophic Zone, the latter zone denoted by massive siltstones. (10, 11) The massive siltstone rock represented at the onset of the Heterotrophic Zone continues through (10) the lower channel in box 12, and the end of this zone in (11) the middle channel of box 12 is characterized with siltstone rocks infiltrated with deposits of siliceous nodules. (12, 13) Eunotioid diatoms and acidic chrysophytes reappear in (12) the upper channel of box 12 where the rock transitions back to dark organic mudstone, and these organisms remain throughout most of (13) box 11 until the end of the lake phase.

et al., 1990). *Actinella* taxa are overwhelmingly reported from highly acidic habitats with high concentrations of dissolved humic substances, and almost exclusively from tropical regions (Kocielek and Rhode, 1998; Sabbe et al., 2001; Metzeltin and Lange-Bertalot, 2007; Melo et al., 2010; Siver et al., 2010, 2015). Flower (1989) and Kingston (2003) reported *Oxyneis* taxa as indicators of lakes, including bogs, with pH <5 and low in nutrients (Patrick and Reimer, 1966; Siver and Hamilton, 2011). In summary, the totality of microfossil evidence, coupled with the dark and organic-rich mudstones characterizing the Eunotioid Zone, clearly infers a shallow, acidic, dystrophic environment that was low in nutrients. Given that the zone occurs in >13 m of the core, we estimated that it may have lasted over 10,000 years.

As was observed between the *Botryococcus* and *Aulacoseira* zones, sudden changes in organisms and character of the core material marked a distinct and rapid transition from the Eunotioid Zone to the Heterotrophic Zone. The transition was marked by the virtual disappearance of all photosynthetic scaled chrysophytes and diatoms, and replacement with silica scale-bearing heterotrophic protists dominated by heliozoans and paraphysomonads. Heliozoans can grow and thrive in either the plankton or attached to substrates, including on detritus, sediments, and aquatic plants, and their preferred food source is small algal cells (Laybourn-Parry et al., 1990, 1991; Zimmermann et al., 1996). The highest concentrations of heliozoans are typically found under mesoeutrophic to highly eutrophic conditions, with abundances positively correlated with chlorophyll concentrations (Arndt, 1993; Mathes and Arndt, 1994; Zimmermann et al., 1996). Higher temperatures also yield greater numbers of heliozoans. Like heliozoans, the highest concentrations and diversities of paraphysomonads are also associated with eutrophic conditions (Finlay and Clarke, 1999; Esteban et al., 2012). Based on these studies, the transition to the Heterotrophic Zone was probably linked to a sudden increase in trophic condition. The declines of eunotioid species and scaled chrysophytes further infer an increase in pH. Interestingly, concentrations of heliozoans can be reduced considerably through predation by metazooplankton and larger ciliates (Stensdotter-Blomberg, 1998), while smaller ciliates can serve as prey for some heliozoans (Pierce and Coats, 1999). We can't comment on potential predator-prey interactions of heliozoans with other heterotrophic protists in the Giraffe waterbody, but declines in scaled chrysophytes and diatoms imply that other groups of algae (e.g., greens and cryptomonads) and cyanobacteria were likely food sources for the heliozoans.

The uppermost and final four meters of the lacustrine phase, the Terminal Lake Zone, represents transition of the waterbody

to a terrestrial ecosystem. This zone is represented by a reemergence of scaled chrysophytes, eunotioid diatoms, and testate amoebae, coupled with significant declines in heliozoans and paraphysomonads. Collectively, these changes infer a shift back to an acidic waterbody, with elevated levels of dissolved humic matter and low to moderate nutrient content. Interestingly, in many respects, the composition of microfossils in the Terminal Lake Zone is most similar to an earlier time period represented by samples in box 23, both with high numbers of testates, *Mallomonas insignis*, *M. asmundiae*, and *M. bangladeschica*. However, eunotioid diatoms were not important components of the community represented in box 23. Still, the similarities further support the hypothesis that the waterbody was indeed shallow in its early history.

Conclusions

The Giraffe Pipe locality provides an important window into a freshwater environment situated near the Arctic Circle under a warm greenhouse climate. The site harbors an unprecedented treasure trove of exquisitely preserved fossils of protists, including chrysophytes, diatoms, euglyphids, rotosphaerids, heliozoans, and paraphysomonads, as well as sponges and plant remains. Giraffe Pipe microfossils provide geologic age constraints for multiple eukaryotic lineages, and represent the oldest known records for many of the organisms uncovered. Our initial hypothesis that the waterbody commenced as a deep maar lake and slowly filled over time eventually becoming a wetland was proven incorrect. Instead, the waterbody presented a series of successive shallow environments for most of its history, including at its inception, each correlated with changes in lakewater chemistry. The detailed paleontological database developed as part of this study can serve as a baseline for a complementary study of the geochemical and sedimentological details of the core, which collectively should provide additional clues on lake history, including potential effects of shifting climate conditions. Given the preservation qualities and rich diversity of the fossil remains at the Giraffe Pipe locality, additional core material, and certainly a full excavation of the site, would undoubtedly uncover a wealth of new evolutionary history, and further broaden our knowledge of the warm Eocene Arctic.

Acknowledgments

This project was funded, in part, with grants to PAS from the National Science Foundation (DEB-0716606, DEB-1144098,

EAR-1725265, and EAR-1940070). We thank J. Romanow and X. Sun from the Bioscience Electron Microscopy Laboratory (BEML) at the University of Connecticut for help with SEM facilities. We also thank the many students who helped with sample preparation over the years, especially A. Barber and W. Karis, and helpful suggestions from two anonymous reviewers. Special thanks to our colleague A.P. Wolfe for many insightful discussions over the years.

Declaration of competing interests

The authors declare none.

Data availability statement

Data available from the Dryad Repository: <https://doi.org/10.5061/dryad.djh9w0w3s>.

References

- Amesbury, M.J., Booth, R.K., Roland, T.P., Bunbury, J., Clifford, M.J., Charman, D.J., Elliot, S., Finkelstein, S., Garneau, M., Hughes, P.D.M., Lamar, A., Loisel, J., Mackay, H., Magnan, G., Markel, E.R., Mitchell, E.A.D., Payne, R.J., Pelletier, N., Roe, H., Sullivan, M.E., Swindles, G.T., Talbot, J., van Belen, S., and Wamer, B.G., 2018, Towards a Holarctic synthesis of peatland testate amoeba ecology: development of a new continental-scale palaeohydrological transfer function for North America and comparison to European data: *Quaternary Science Reviews*, v. 201, p. 483–500.
- Archibald, S.B., Johnson, K.R., Mathewes, R.W., and Greenwood, D.R., 2011, Intercontinental dispersal of giant thermophilic ants across the Arctic during early Eocene hyperthermals: *Proceedings of the Royal Society B*, v. 278, p. 3679–3686.
- Arndt, H., 1993, A critical review of the importance of rhizopods (naked and testate amoebae) and actinopods (heliozoa) in lake plankton: *Marine Microbial Food Webs*, v. 7, p. 3–29.
- Barber, A., Siver, P.A., and Karis, W., 2013, Euglyphid testate amoebae (Rhizaria: Euglyphida) from an Arctic Eocene waterbody: evidence of evolutionary stasis in plate morphology for over 40 million years: *Protist*, v. 164, p. 541–555.
- Barral, A., Gomez, B., Fourel, F., Daviero-Gomez, V., and Lécuyer, C., 2017, CO₂ and temperature decoupling at the million-year scale during the Cretaceous Greenhouse: *Scientific Reports*, v. 7, 8310. <https://doi.org/10.1038/s41598-017-08234-0>.
- Battisti, D.S., and Naylor, R.L., 2009, Historical warnings of future food insecurity with unprecedented seasonal heat: *Science*, v. 323, p. 240–244.
- Bhatti, S., and Colman, B., 2005, Inorganic carbon acquisition by the chrysophyte *Mallomonas pusilla*: *Canadian Journal of Botany*, v. 83, p. 891–897.
- Boeff, K.A., Strock, K.E., and Saros, J.E., 2016, Evaluating planktonic diatom response to climate change across three lakes with differing morphometry: *Journal of Paleolimnology*, v. 56, p. 33–47.
- Booth, R.K., 2002, Testate amoebae as paleoindicators of surface moisture changes on Michigan peatlands: modern ecology and hydrological calibration: *Journal of Paleolimnology*, v. 28, p. 329–348.
- Camburn, K.E., and Charles, D.F., 2000, Diatoms of low-alkalinity lakes in the northeastern United States: The Academy of Natural Sciences of Philadelphia, Special Publication 18, 152 p.
- Clarke, K.R., and Warwick, R.M., 2001, Change in Marine Communities: An Approach to Statistical Analysis and Interpretation, 2nd Edition: PRIMER-E, Ltd., Plymouth Marine Laboratory, Plymouth, UK.
- Clarke, K.R., Gorley, R.N., Somerfield, P.J., and Warwick, R.M., 2014, Change in Marine Communities: An Approach to Statistical Analysis and Interpretation, 3rd Edition: PRIMER-E, Plymouth, UK.
- Clyde, W.C., and Gingerich, P.D., 1998, Mammalian community response to the latest Paleocene thermal maximum: an isotaphonomic study in the northern Bighorn Basin, Wyoming: *Geology*, v. 26, p. 1011–1014.
- Cohen J., Screen, J.A., Furtado, J.C., Barlow, M., Whittleston, D., Coumou, D., Francis, J., Dethloff, K., Entekhabi, D., Overland, J., and Jones, J., 2014, Recent arctic amplification and extreme mid-latitude weather: *Nature Geoscience*, v. 7, p. 627–637.
- Colby, G.A., Ruuskanen, M.O., St. Pierre, K.A., St. Louis, V.L., Poulain, A.J., and Aris-Brosou, S., 2020, Warming climate is reducing the diversity of dominant microbes in the largest high Arctic lake: *Frontiers in Microbiology*, v. 11. <https://doi.org/10.3389/fmicb.2020.561194>.
- Conrad, W., 1938, Notes protistologiques I. *Mallomonas lichenensis* n. sp.: *Bulletin du Musée Royal d'histoire Naturelle de Belgique*, v. 14, p. 1–4.
- Creaser, R., Grütter, H., Carlson, J., and Crawford, B., 2004, Macrocristal phlogopite Rb-Sr dates for the Ekati Property kimberlites, Slave Province, Canada: evidence for multiple intrusive episodes in the Paleocene and Eocene: *Lithos*, v. 76, p. 399–414.
- Cronberg, G., and Kristiansen, J., 1980, Synuraceae and other Chrysophyceae from central Smaland, Sweden: *Botaniska Notiser*, v. 133, p. 595–618.
- Cumming, B.F., Smol, J.P., Kingston, J.C., Charles, D.F., Birks, H.J.B., Camburn, K.E., Dixit, S.S., Uutala, A.J., and Selle, A.R., 1992, How much acidification has occurred in Adirondack region lakes (New York, USA) since preindustrial times?: *Canadian Journal of Fisheries and Aquatic Sciences*, v. 49, p. 128–141.
- Cumming, B.F., Davey, K.A., Smol, J.P., and Birks, H.J.B., 1994, When did acid-sensitive Adirondack lakes (New York, USA) begin to acidify and are they still acidifying?: *Canadian Journal of Fisheries and Aquatic Sciences*, v. 51, p. 1550–1568.
- Dawson, M.R., McKenna, M.C., Beard, K.C., and Hutchison, J.H., 1993, An early Eocene plagiomenid mammal from Ellesmere and Axel Heiberg islands, Arctic Canada: *Kaupi*, v. 3, p. 179–192.
- Diffenbaugh, N.S., and Field, C.B., 2013, Changes in ecologically critical terrestrial climate conditions: *Science*, v. 341, p. 486–492.
- Doria, G., Royer, D.L., Wolfe, A.P., Fox, A., Westgate, J.A., and Beerling, D.J., 2011, Declining atmospheric CO₂ during the late middle Eocene climate transition: *American Journal of Science*, v. 3, p. 63–75.
- Douglas, M.S.V., and Smol, J.P., 1995, Paleolimnological significance of observed distribution patterns of chrysophyte cysts in Arctic pond environments: *Journal of Paleolimnology*, v. 13, p. 79–83.
- Eberle, J.J., 2005, A new ‘tapir’ from Ellesmere Island—implications for northern high latitude paleobiogeography and tapir paleobiology: *Palaeogeography, Palaeoclimatology, Palaeoecology*, v. 227, p. 311–322.
- Eberle, J.J., and Greenwood, D.R., 2012, Life at the top of the greenhouse Eocene world—a review of the Eocene flora and vertebrate fauna from Canada’s high Arctic: *Geological Society of America Bulletin*, v. 124, p. 3–23.
- Eberle, J.J., Fricke, H.C., Humphrey, J.D., Hackett, L., Newbrey, M.G., and Hutchison, J.H., 2010, Seasonal variability in arctic temperatures during early Eocene time: *Earth and Planetary Science Letters*, v. 296, p. 481–486.
- Edlund, M.B., Stoermer, E.F., and Taylor, C.M., 1996, *Aulacoseira skvortzowii* sp. nov. (Bacillariophyta), a poorly understood diatom from Lake Baikal, Russia: *Journal of Phycology*, v. 32, p. 165–175.
- Ehrenberg, C.G., 1834, Beiträge zur physiologischen Kenntniss der Corallenthiere im allgemeinen, und besonders des rothen Meeres, nebst einem Versuche zur physiologischen Systematik derselben. I. Abhandlungen der Königlichen Akademie Wissenschaften zu Berlin: *Physikalische Klasse*, v. 1832, p. 225–380.
- Eloranta, P., 1989, Scaled chrysophytes (Chrysophyceae and Synurophyceae) from national park lakes in southern and central Finland: *Nordic Journal of Botany*, v. 8, p. 67–81.
- Escobar, J., Brenner, M., Whitmore, T.J., Kenney, W., and Curtis, J., 2008, Ecology of testate amoebae (thecamoebians) in subtropical Florida lakes: *Journal of Paleolimnology*, v. 40, p. 715–731.
- Esteban, G.F., Finlay, B.J., and Clarke, K.J., 2012, Priest Pot in the English Lake District: a showcase of microbial diversity: *Freshwater Biology*, v. 57, p. 321–330.
- Estes, R., and Hutchison, J.H., 1980, Eocene lower vertebrates from Ellesmere Island, Canadian Arctic Archipelago: *Palaeogeography, Palaeoclimatology, Palaeoecology*, v. 30, p. 325–347.
- Finlay, B.J., and Clarke, K.J., 1999, Apparent global ubiquity of species in the protist genus *Paraphysomonas*: *Protist*, v. 150, p. 419–430.
- Flower, R.J., 1989, A new variety of *Tabellaria binalis* (Ehrenb.) Grunow from several acid lakes in the U.K.: *Diatom Research*, v. 4, p. 21–23.
- Foissner, W., 2006, Biogeography and dispersal of micro-organisms: a review emphasizing protists: *Acta Protozoologica*, v. 45, p. 111–136.
- Gaiser, E.E., and Johansen, J., 2000, Freshwater diatoms from Carolina bays and other isolated wetlands on the Atlantic coastal plain of South Carolina, U.S.A., with descriptions of seven taxa new to science: *Diatom Research*, v. 15, p. 75–130.
- Greenwood, D.R., Basinger, J.F., and Smith, R.Y., 2010, How wet was the Arctic Eocene rain forest? Estimates of precipitation from Paleogene Arctic macrofloras: *Geology*, v. 38, p. 15–18.
- Guy-Ohlson, D., 1992, *Botryococcus* as an aid in the interpretation of paleo-environment and depositional processes: *Review of Paleobotany and Palynology*, v. 71, p. 1–15.
- Hadley, K.R., Paterson, A.M., Rühland, K.M., White, H., Wolfe, B.B., Keller, W., and Smol, J.P., 2019, Biological and geochemical changes in shallow

- lakes of the Hudson Bay Lowlands: a response to recent warming: *Journal of Paleolimnology*, v. 61, p. 313–328.
- Hickey L.J., West, R.M., Dawson, M.R., and Choi, D.K., 1983, Arctic terrestrial biota: paleomagnetic evidence of age disparity with mid-northern latitudes during the Late Cretaceous and early Tertiary: *Science*, v. 221, p. 1153–1156.
- Hobbie, J.E., Peterson, B.J., Bettez, N., Deegan, L., O'Brien, W.J., Kling, G.W., Kipphut, G.W., and Bowden, W.B., 1999, Impact on global change on the biogeochemistry and ecosystems of an Arctic freshwater system: *Polar Research*, v. 18, p. 207–214.
- Houk, V., and Klee, R., 2007, Atlas of freshwater centric diatoms with a brief key and descriptions. Part II. Melosiraceae and Aulacoseiraceae (Supplement to Part I): *Czech Phycology Supplement*, v. 1, p. 1–112.
- IPCC [Intergovernmental Panel on Climate Change], 2019, IPCC Special Report on the Ocean and Cryosphere in a Changing Climate [Pörtner, H.-O., Roberts, D.C., Masson-Delmotte, V., Zhai, P., Tignor, M., Poloczanska, E., Mintenbeck, K., Alegria, A., Nicolai, M., Okem, A., Petzold, J., Rama, B., and Weyer, N.M., eds.]: Cambridge, UK and New York, Cambridge University Press, 755 p.
- Jahren, A.H., 2007, The Arctic forest of the middle Eocene: *Annual Review of Earth and Planetary Sciences*, v. 35, p. 509–540.
- Jewson, D.H., Granin, N.G., Zhdanov, A.A., Gorbunova, L.A., Bondarenko, N.A., and Gnatovsky, R.Y., 2008, Resting stages and ecology of the planktonic diatom *Aulacoserira skvortzowii* in Lake Baikal: *Limnology and Oceanography*, v. 53, p. 1125–1136.
- Kattson, V.M., and Källén, E., 2005, Future climate change: modeling and scenarios for the Arctic, in ACIA, Arctic Climate Impact Assessment: Cambridge, Cambridge University Press, p. 99–150.
- Kingston, J.C., 2003, Araphid and monoraphid diatoms, in Wehr, J.D., and Sheath, R.G., eds., *Freshwater Algae of North America*: New York, Academic Press, p. 595–636.
- Kociolek, J.P., and Rhode, K., 1998, Raphe vestiges in “*Asterionella*” species from Madagascar: evidence for a polyphyletic origin of the araphid diatoms?: *Cryptogamie Algologie*, v. 19, p. 57–74.
- Korshikov, A.A., 1929, Studies on the Chryomonads. I: *Archiv für Protistenkunde*, v. 67, p. 253–290.
- Kristiansen, J., 2005, Golden Algae: A Biology of Chrysophytes: Königstein, Germany, Koeltz Scientific Books, 167 p.
- Kristiansen, J., Düwel, L., and Wegeberg, S., 1997, Silica-scaled chrysophytes from the Taymyr Peninsula, Northern Siberia: *Nova Hedwigia*, v. 65, p. 337–351.
- Kritzberg, E.S., and Ekström, S.M., 2012, Increasing iron concentrations in surface waters—a factor behind brownification?: *Biogeosciences*, v. 9, p. 1465–1478.
- Laybourn-Parry, J., Olver, J., Rogerson, A., and Duverge, P.L., 1990, The temporal and spatial patterns of protozooplankton abundance in a eutrophic temperate lake: *Hydrobiologia*, v. 203, p. 99–110.
- Laybourn-Parry, J., Marchant, H.J., and Brown, P., 1991, The plankton of a large oligotrophic freshwater Antarctic lake: *Journal of Plankton Research*, v. 13, p. 1137–1149.
- Li, Y.M., Ferguson, D.K., Wang, Y.F., and Li, C.S., 2010, Paleoenvironmental inferences from diatom assemblages of the middle Miocene Shanwang Formation, Shandong, China: *Journal of Paleolimnology*, v. 43, p. 799–814.
- Lu, J., and Cai, M., 2009, Seasonality of polar surface warming amplification in climate simulations: *Geophysical Research Letters*, v. 36, L16704. <https://doi.org/10.1029/2009GL040133>.
- Lunt, D.J., Haywood, A.M., Schmidt, G.A., Salzmann, U., Valdes, P., and Dowsett, H., 2010, Earth system sensitivity inferred from Pliocene modeling and data: *Nature Geoscience*, v. 3, p. 60–64.
- Lunt, D.J., Dunkley Jones, T., Heinemann, M., Huber, M., LeGrande, A., Winguth, A., Loptson, C., Marotzke, J., Roberts, C.D., Tindall, J., Valdes, P., and Winguth, C., 2012, A model-data comparison for a multi-model ensemble of early Eocene atmosphere-ocean simulations: *EoMIP: Climate of the Past*, v. 8, p. 1717–1736.
- Marsicano, L.J., and Siver, P.A., 1993, A paleolimnological assessment of lake acidification in five Connecticut lakes: *Journal of Paleolimnology*, v. 9, p. 209–221.
- Mathes, J., and Arndt, H., 1994, Biomass and composition of protozooplankton in relation to lake trophy in north German lakes: *Marine Microbial Food Webs*, v. 8, p. 357–375.
- McIver, E.E., and Basinger, J.F., 1999, Early Tertiary floral evolution in the Canadian High Arctic: *Annals of the Missouri Botanical Garden*, v. 86, p. 523–545.
- McKeown, M.M., Wilmshurst, J.M., Duckert, C., Wood, J.R., and Mitchell, E.A.D., 2019, Assessing the ecological value of small testate amoebae (<45 µm) in New Zealand peatlands: *European Journal of Protistology*, v. 68, p. 1–16.
- Melo, S., Torgan, L.C. and Raupp, S.V., 2010, *Actinella* species (Bacillariophyta) from an Amazon blackwater floodplain lake (Amazonas-Brazil): *Acta Amazonica*, v. 40, p. 269–274.
- Metzeltin, D., and Lange-Bertalot, H., 1998, Tropical diatoms of South America I: *Iconographia Diatomologica*, v. 5, p. 1–695.
- Metzeltin D., and Lange-Bertalot, H., 2007, Tropical diatoms of South America. II. Special remarks on biogeographic disjunction: *Iconographia Diatomologica*, v. 18, p. 1–877.
- Mitchell, E.A.D., Buttler, A., Warner, B.G., and Gobat, J.M., 1999, Ecology of testate amoebae (Protozoa: Rhizopoda) in sphagnum peatlands in the Jura Mountains, Switzerland and France: *Ecoscience*, v. 6, p. 565–576.
- Mitchell, E.A.D., Charman, D.J., and Warner, B.G., 2008, Testate amoebae analysis in ecological and paleoecological studies of wetlands: past, present and future: *Biodiversity and Conservation*, v. 17, p. 2115–2137.
- Nicholls, K.H., 1982, *Mallomonas* species (Chrysophyceae) from Ontario, Canada, including descriptions of two new species: *Nova Hedwigia*, v. 36, p. 89–112.
- Nicholls, K.H., and Wujek, D.E., 2015, Chrysophycean algae, in Wehr, J.D., Sheath, R.G., and Kociolek, J.P., eds., *Freshwater Algae of North America: Ecology and Classification*, 2nd ed.: San Diego, California, Academic Press, p. 605–650.
- Notz, D., and Stroeve, J., 2018, The trajectory towards a seasonally ice-free Arctic Ocean: *Current Climate Change Reports*, v. 4, p. 407–416.
- Ogden, C.G., and Hedley, R.H., 1980, *An Atlas of Freshwater Testate Amoebae*: London and Oxford, UK, British Museum of Natural History and Oxford University Press, 222 p.
- Pace, M.L., and Cole, J.J., 2002, Synchronous variation of dissolved organic carbon and color in lakes: *Limnology and Oceanography*, v. 47, p. 333–342.
- Pagani, M., Huber, M., and Sageman, B., 2014, Greenhouse climates, in Turekian, K., and Holland, H., eds., *Treatise on Geochemistry*, 2nd ed.: Chicago, Elsevier, p. 281–304.
- Patrick, R., and Reimer, C.W., 1966, *The Diatoms of the United States: Fragilariaceae, Eunotiaceae, Achnantheaceae, Naviculaceae*: Philadelphia, Academy of Natural Sciences of Philadelphia, v. 1, 688 p.
- Patterson, R.T., Roe, H.M., and Swindles, G.T., 2012, Development of an Arcellacea (testate lobose amoebae) based transfer function for sedimentary phosphorus in lakes: *Palaeogeography, Palaeoclimatology, Palaeoecology*, v. 348–349, p. 32–44.
- Penard, E., 1919, *Mallomonas insignis* spec. nov.?: *Bulletin de la Société Botanique Genève*, v. 2, sér. 11, p. 122–128.
- Petersen, J.B., and Hansen, J.B., 1956, On the scales of some *Synura* species: *Biologiske Meddelelser*, v. 23, p. 3–27.
- Pierce, R.W., and Coats, D.W., 1999, The feeding ecology of *Actinophrys sol* (Sarcodina: Heliozoa) in Chesapeake Bay: *Journal of Eukaryote Microbiology*, v. 46, p. 451–457.
- Pisera, A., Siver, P.A., and Wolfe, A.P., 2013, A first account of freshwater potamoledid sponges (Demospongiae, Spongillina, Potamoledidae) from the middle Eocene: biogeographic and paleoclimatic implications: *Journal of Paleontology*, v. 87, p. 373–378.
- Pisera, A., Manconi, R., Siver, P.A., and Wolfe, A.P., 2016, The sponge genus *Ephydatia* from the middle Eocene Giraffe Pipe kimberlite diatreme lake: environmental and evolutionary significance: *Paläontologische Zeitschrift*, v. 90, p. 673–680.
- Raven, J.A., Ball, L.A., Beardall, J., Giordano, M., and Maberly, S.C., 2005, Algae lacking carbon concentrating mechanisms: *Canadian Journal of Botany*, v. 83, p. 879–890.
- Raven, J.A., Giordano, M., Beardall, J., and Maberly, S.C., 2012, Algal evolution in relation to atmospheric CO₂: carboxylases, carbon-concentrating mechanisms and carbon oxidation cycles: *Philosophical Transactions of the Royal Society B*, v. 367, p. 493–507.
- Reyes, A., Andersen, B., Bolton, M., Buryak, S., Madsen, F., Davies, J., Koppellhus, E., Royer, D., Siver, P.A., and Tierney, J., 2020, Prospects, pitfalls, and pitfalls of high latitude paleoenvironmental reconstruction from the post-eruptive sedimentary fill of kimberlite pipes in northern Canada: *Geological Society of America Abstracts with Programs*, v. 52, no. 6. <https://doi.org/10.1130/abs/2020AM-358957>.
- Richardson, K., Steffen, W., Liverman, D., Barker, T., Jotzo, F., Kammen, D., Leemans, R., Lenton, T., Munasinghe, M., Osman-Elasha, B., Schellnhuber, H.J., Stern, N., Vogel, C., and Waever, O., 2011, *Climate Change: Global Risks, Challenges and Decisions*: Cambridge, Cambridge University Press, 40 p.
- Rojackers, R.M.M., and Siemensma, F.J., 1988, A study of cristidiscoid amoebae (Rhizopoda, Filosea), with descriptions of new species and keys to genera and species: *Archiv für Protistenkunde*, v. 135, p. 237–253.
- Round, F.E., Crawford, R.M., and Mann, D.G., 1990, *The Diatoms. Biology and Morphology of the Genera*: Cambridge, Cambridge University Press, 747 p.
- Sabbe, K., Vanhoutte, K., Lowe, R.L., Bergey, E.A., Biggs, B.J.F., Francoeur, S., Hodgson, D., and Vyverman, W., 2001, Six new *Actinella* (Bacillariophyta) species from Papua New Guinea, Australia and New Zealand: further evidence for widespread diatom endemism in the Australasian region: *European Journal of Phycology*, v. 36, p. 321–340.

- Saros, J.E., Northington, R.M., Osburn, C.L., Burpee, B.T., and Anderson, N.J., 2016, Thermal stratification in small Arctic lakes of southwest Greenland affected by water transparency and epilimnetic temperatures: *Limnology and Oceanography*, v. 61, p. 1530–1542.
- Schindler, D.W., and Smol, J.P., 2006, Cumulative effects of climate warming and other human activities on freshwaters of arctic and subarctic North America: *Ambio*, v. 35, p. 160–168.
- Schmitz, B., and Pujalte, V., 2007, Abrupt increase in seasonal extreme precipitation at the Paleocene-Eocene boundary: *Geology*, v. 35, p. 215–218.
- Schubert, B.A., Jahren, A.H., Eberle, J.J., Sternberg, L.S.L., and Eberth, D.A., 2012, A summertime rainy season in the Arctic forests of the Eocene: *Geology*, v. 40, p. 523–526.
- Screen, J.A., and Simmonds, I., 2010, The central role of diminishing sea ice in recent arctic temperature amplification: *Nature*, v. 464, p. 1334–337.
- Seidel, D.J., Fu, Q., Randel, W.J., and Reichler, T.J., 2008, Widening of the tropical belt in a changing climate: *Nature Geoscience*, v. 1, p. 21–24.
- Sereze, M.C., and Barry, R.G., 2011, Processes and impacts of arctic amplification: a research synthesis: *Global and Planetary Change*, v. 77, p. 85–96.
- Sereze, M.C., and Francis, J.A., 2006, The arctic amplification debate: *Climatic Change*, v. 76, p. 241–264.
- Siemasma, F.J., 1981, De Nederlandse Zonnediertjes (Actinopoda, Heliozoa): Wetenschappelijke Mededelingen van de KNNV, v. 149, 118 p.
- Siver, P.A., 1989, The distribution of scaled chrysophytes along a pH gradient: *Canadian Journal of Botany*, v. 67, p. 2120–2130.
- Siver, P.A., 1995, The distribution of chrysophytes along environmental gradients: their use as biological indicators, in Sandgren, C., Smol, J., and Kristiansen, J., eds., *Chrysophyte Algae: Ecology, Phylogeny and Development*: Cambridge, Cambridge University Press, p. 232–268.
- Siver, P.A., 2013, *Synura cronbergiae* sp. nov., a new species described from two Paleogene maar lakes in northern Canada: *Nova Hedwigia*, v. 97, p. 179–187.
- Siver, P.A., 2015, The Synurophyceae, in Wehr, J.D., Sheath, R.G., and Kociolek, J.P., eds., *Freshwater Algae of North America: Ecology and Classification*, 2nd ed.: San Diego, California, Academic Press, p. 605–650.
- Siver, P.A., 2018, *Mallomonas aperturae* sp. nov. (Synurophyceae) reveals that the complex cell architecture observed on modern synurophytes was well established by the middle Eocene: *Phycologia*, v. 57, p. 273–279.
- Siver, P.A., 2020, Remarkably preserved cysts of the extinct synurophyte, *Mallomonas ampla*, uncovered from a 48 Ma freshwater Eocene lake: *Nature Special Reports*, v. 10, 5204. <https://doi.org/10.1038/s41598-020-61993-1>.
- Siver, P.A., 2021, *Aulacoseira chockii* sp. nov., an early freshwater centric diatom from the Eocene bearing a unique morphology: *Diatom Research*, v. 36, p. 253–263.
- Siver, P.A., and Hamer, J.S., 1989, Multivariate statistical analysis of the factors controlling the distribution of scaled chrysophytes: *Limnology and Oceanography*, v. 34, p. 368–381.
- Siver, P.A., and Hamilton, P.B., 2011, Diatoms of North America: The Freshwater Flora of the Atlantic Coastal Plain: *Iconographia Diatomologica*, v. 22, 920 p.
- Siver, P.A., and Kling, H., 1997, Morphological observations of *Aulacoseira* using scanning electron microscopy: *Canadian Journal of Botany*, v. 75, p. 1807–1835.
- Siver, P.A., and Lott, A.M., 2012, Do scaled chrysophytes have a biogeography? Evidence from the east coast of North America: *Freshwater Biology*, v. 57, p. 451–467.
- Siver, P.A., and Skogstad, A., 2022, A first account of the heterotrophic eukaryote *Rabdiorhynchus* Rainer from the fossil record and description of a new species from an ancient Eocene Arctic freshwater lake: *European Journal of Protistology*, v. 82, 125857. <https://doi.org/10.1016/j.ejop.2021.125857>.
- Siver, P.A., and Wolfe, A.P., 2005a, Eocene scaled chrysophytes with pronounced modern affinities: *International Journal of Plant Sciences*, v. 166, p. 533–536.
- Siver, P.A., and Wolfe, A.P., 2005b, Scaled chrysophytes in middle Eocene lake sediments from Northwestern Canada, including descriptions of six new species: *Nova Hedwigia*, Beiheft, v. 128, p. 295–308.
- Siver, P.A., and Wolfe, A.P., 2009, Tropical ochrophyte algae from the Eocene of northern Canada: a biogeographic response to past global warming: *Palaios*, v. 24, p. 192–198.
- Siver, P.A., Hamilton, P.B., Stachura-Suchoples, K., and Kociolek, J.P., 2005, Diatoms of North America: The Freshwater Flora of Cape Cod: *Iconographia Diatomologica*, v. 14, 463 p.
- Siver, P.A., Wolfe, A.P., and Edlund, M., 2010, Taxonomic descriptions and evolutionary implications of middle Eocene pennate diatoms representing the extant genera *Oxyneis*, *Actinella* and *Nupela* (Bacillariophyceae): *Plant Ecology and Evolution*, v. 143, p. 340–351.
- Siver, P.A., Bishop, J., Lott, A.M., and Wolfe, A.P., 2015, Heteropolar eunotioid diatoms (Bacillariophyceae) were common in the North American Arctic during the middle Eocene: *Journal of Micropaleontology*, v. 34, p. 151–163.
- Siver, P.A., Wolfe, A.P., Edlund, M.B., Sibley, J., Hausman, J., Torres, P., and Lott, A.M., 2019, *Aulacoseira giraffensis* (Bacillariophyceae), a new diatom species forming massive populations in an Eocene lake: *Plant Ecology and Evolution*, v. 152, p. 358–367.
- Siver, P.A., Lott, A.M., and Torres, P., 2020, Abundance and distribution of testate amoebae bearing siliceous plates in freshwater lakes and ponds along the east coast of North America: importance of water depth and pH: *Freshwater Science*, v. 39, p. 791–803.
- Sluijs A., Pross, J., and Brinkhuis, H., 2005, From greenhouse to icehouse: organic-walled dinoflagellate cysts as paleoenvironmental indicators in the Paleogene: *Earth-Science Reviews*, v. 68, p. 281–315.
- Smittenberg, R.H., Baas, M., Schouten, S., and Sinninghe Damste, J.S., 2005, The demise of the alga *Botryococcus braunii* from a Norwegian fjord was due to early eutrophication: The Holocene, v. 15, p. 133–140.
- Smol, J.P., 1985, The ratio of diatom frustules to chrysophycean statospores: a useful paleolimnological index: *Hydrobiologia*, v. 123, p. 199–208.
- Stager, J.C., Wiltse, B., Cumming, B.F., Messner, T.C., Robtoy, J., and Cushing, S., 2021, Hydroclimatic and cultural instability in northeastern North America during the last millennium: *PLoS ONE*, v. 16, e0248060. <https://doi.org/10.1371/journal.pone.0248060>.
- Stensdotter-Blomberg, U., 1998, Factors controlling pelagic populations of ciliates and heliozoans—late summer investigations in an acidic lake before and after liming: *Journal of Plankton Research*, v. 20, p. 423–442.
- Takahashi, E., and Hayakawa, T., 1979, The Synuraceae (Chrysophyceae) in Bangladesh: *Phykos*, v. 18, p. 129–147.
- Thomsen H.A., 1978, On the identity between the heliozoan *Pinaciophora fluviatilis* and *Potamodiscus kalbei*; with the description of eight new *Pinaciophora* species: *Protistologica*, v. 14, p. 359–373.
- Tripathi, A., Zachos, J., Marinovich, L. Jr., and Bice, K., 2001, Late Paleocene arctic coastal climate inferred from molluscan stable and radiogenic isotope ratios: *Palaeogeography, Palaeoclimatology, Palaeoecology*, v. 170, p. 101–113.
- Tsyganov, A.N., Malysheva, E.A., Zharov, A.A., Sapelko, T.V., and Mazei, Y.A., 2019, Distribution of benthic testate amoeba assemblages along a water depth gradient in freshwater lakes of the Meshchera Lowlands, Russia, and utility of the microfossils for inferring past lake water level: *Journal of Paleolimnology*, v. 62, p. 137–150.
- Tyson, R.V., 1995, Distribution of the palynomorph group: phytoplankton subgroup, chlorococcale algae, in Tyson, R.V., ed., *Sedimentary Organic Matter: Organic Facies and Palynofacies*: London, Chapman and Hall, p. 309–317.
- Ufnar, D.F., Gonzáles, L.A., Ludvigson, G.A., Brenner, R.L., and Witzke, B.J., 2004, Evidence for increased latent heat transport during the Cretaceous (Albian) greenhouse warming: *Geology*, v. 32, p. 1049–1052.
- Vincent, W.F., and Hobbie, J.E., 2000, Ecology of Arctic lakes and rivers, in Nuttal, M. and Callaghan, T., eds., *The Arctic: Environment, People, Policies*: London, Harwood Academic Publishers, p. 197–232.
- Westerhold, T., Röhl, U., Frederichs, T., Bohaty, S.M., and Zachos, J.C., 2015, Astronomical calibration of the geological timescale: closing the middle Eocene gap: *Climate of the Past*, v. 11, p. 1181–1195.
- Westerhold, T., Marwan, N., Drury, A.J., Liebrand, D., Agnini, C., Anagnostou, E., Barnet, J.S.K., Bohaty, S.M., de Vleeschouwer, D., Florindo, F., Frederichs, T., Hodell, D.A., Holbourn, A.E., Kroon, D., Lauretano, V., Littler, K., Lourens, L.J., Lyle, M., Palike, H., Rohl, U., Tian, J., Wilkens, R.H., Wilson, P.A., and Zachos, J.C., 2020, An astronomically dated record of Earth's climate and its predictability over the last 66 million years: *Science*, v. 369, p. 1383–1387.
- Wing, S.L., Alroy, J., and Hickey, L.J., 1995, Plant and mammal diversity in the Paleocene to early Eocene of the Bighorn Basin: *Palaeogeography, Palaeoclimatology, Palaeoecology*, v. 115, p. 117–155.
- Wolfe, A.P., 2002, Climate modulates the acidity of Arctic lakes on millennial time scales: *Geology*, v. 30, p. 215–218.
- Wolfe, A.P., and Perren, B.B., 2001, Chrysophyte microfossils record marked responses to recent environmental changes in high- and mid-Arctic lakes: *Canadian Journal of Botany*, v. 79, p. 747–752.
- Wolfe, A.P., and Siver, P.A., 2009, Three genera of extant thalassiosiroid diatoms from middle Eocene lake sediments in northern Canada: *American Journal of Botany*, v. 96, p. 487–497.
- Wolfe, A.P., and Siver, P.A., 2013, A hypothesis linking chrysophyte microfossils to lake carbon dynamics on ecological and evolutionary time scales: *Global and Planetary Change*, v. 111, p. 189–198.
- Wolfe, A.P., Edlund, M.B., Sweet, A.R., and Creighton, S., 2006, A first account of organelle preservation in Eocene nonmarine diatoms: observations and paleobiological implications: *Palaios*, v. 21, p. 298–304.
- Wolfe, A.P., Reyes, A.V., Royer, D.L., Greenwood, D.R., Doria, G., Gagen, M.H., Siver, P.A., and Westgate, J.A., 2017, Middle Eocene CO₂ and climate reconstructed from the sediment fill of a subarctic kimberlite maar: *Geology*, v. 45, p. 619–622.

- Wrona, F.J., Prowse, T.D., and Reist, J.D., 2005, Ecosystems, in ACIA, Arctic Climate Impact Assessment: Cambridge, Cambridge University Press, p. 60–83.
- Wrona, F.J., Prowse, T.D., Reist, J.D., Hobbie, J.E., Levesque, L.M.J., and Vincent, W.F., 2006, Climate change effects on aquatic biota, ecosystem structure and function: *Ambio*, v. 35, p. 359–369.
- Wujek, D.E., and Timpano, P., 1984, The genus *Mallomonopsis* in the United States: *Transactions of the Kansas Academy of Science*, v. 87, p. 73–82.
- Wujek, D.E., and Van der Veer, J., 1976, Scaled chrysophytes from the Netherlands including a description of a new variety: *Acta Botanica Neerlandica*, v. 25, p. 179–190.
- Zachos, J.C., Pagani, M., Sloan, L., Thomas, E., and Billups, K., 2001, Trends, rhythms, and aberrations in global climate 65 Ma to present: *Science*, v. 292, p. 686–693.
- Zachos, J.C., Dickens, G.R., and Zeebe, R.E., 2008, An early Cenozoic perspective on greenhouse warming and carbon-cycle dynamics: *Nature*, v. 451, p. 279–283.
- Zimmermann, U., Müller, H., and Weisse, T., 1996, Seasonal and spatial variability of planktonic heliozoa in Lake Constance: *Aquatic Microbial Ecology*, v. 11, p. 21–29.

Accepted: 7 October 2022